Biomass Conversion and Biorefinery (2023) 13:977–998
https://doi.org/10.1007/s13399-020-01178-y

ORIGINAL ARTICLE

Techno-economic modeling of an integrated biomethane-biomethanol production process via biomass gasification, electrolysis, biomethanation, and catalytic methanol synthesis

Lorenzo Menin[1] · Vittoria Benedetti[1] · Francesco Patuzzi[1] · Marco Baratieri[1]

Received: 7 September 2020 / Revised: 6 November 2020 / Accepted: 25 November 2020 / Published online: 10 December 2020

Abstract

Biological methanation (biomethanation) of syngas obtained from biomass gasification offers the opportunity to employ a low-pressure, low-temperature process to produce storable bio-derived substitute natural gas (bSNG), although its economic viability is limited by high energy and biomass costs. Research on syngas biomethanation techno-economic performance is limited and novel biomass-to-biomethane process configurations are required in order to assess opportunities for the enhancement of its efficiency and economic feasibility. In this study, we carried out the techno-economic modeling of two processes comprising integrated biomass gasification, electrolysis, and syngas biomethanation with combined heat and power recovery in order to assess and compare their fuel yields, energy efficiency, carbon efficiency, and bSNG minimum selling price (MSP). The first process operates standalone biomethanation (SAB) of syngas and can produce approximately 38,000 Nm^3 of bSNG per day, with a total plant efficiency of 50.6%. The second process (integrated biomethane-biomethanol, IBB) exploits the unconverted carbon stream from the biomethanation process to recover energy and synthesize methanol via direct catalytic CO_2 hydrogenation. In addition to the same bSNG output, the IBB process can produce 10 t/day of biomethanol, at a 99% purity. The IBB process shows little global energy efficiency gains in comparison with SAB (51.7%) due to the large increase in electrolytic hydrogen demand, but it shows a substantial improvement in biomass-to-fuel carbon efficiency (33 vs. 26%). The SAB and IBB processes generate a bSNG MSP of 2.38 €/Nm^3 and 3.68 €/Nm^3, respectively. Hydrogenation of unconverted carbon in biomass-to-biomethane processes comes with high additional capital and operating costs due to the large-scale electrolysis plants required. Consequently, in both processes, the market price gap of the bSNG produced is 0.13 €/kWh_{bSNG} (SAB) and 0.25 €/kWh_{bSNG} (IBB) even under the most optimistic cost scenarios considered, and it is primarily influenced by the cost of surplus electricity utilized in electrolysis, while the selling price of biomethanol exerts a very limited influence on process economics. Intensive subsidization would be required in order to sustain the decentralized production of bSNG through both processes. Despite their limited economic competitiveness, both processes have a size comparable with existing renewable gas production plants in terms of bSNG production capacity and the IBB process is of a size adequate for the supply of biomethanol to a decentralized biorenewable supply chain.

Keywords Biomethanation · Biomethanol · Power-to-gas · Biomass gasification · Techno-economic assessment

Acronyms and symbols

AD	Anaerobic digestion
bSNG	Bio-derived substitute natural gas
bMeOH	Biomethanol
CHP	Combined heat and power
C_{decarb}	Cost of grid gas decarbonization (€/kWh)
daf	Dry and ash free biomass
IBB	Integrated biomethane-biomethanol
IBGEB	Integrated biomass gasification-electrolysis-biomethanation
IBGM	Integrated biomass gasification-methanol synthesis
$LHV_{prod,\ i}$	Lower heating value of product *i* (MJ/kg)

✉ Lorenzo Menin
lmenin@unibz.it

[1] Free University of Bolzano, Bolzano, Italy

LHV_{biom}	Lower heating value of biomass (MJ/kg)
$\dot{m}_{prod,i}$	Mass flow rate of product *i* (kg/s)
Q_i	Heat stream *i* (MW_{th})
W_i	Work stream *i* (MW_{el})
$\dot{n}_{CO2,r.g.}$	Molar flow rate of carbon dioxide in selected reject gases (mol/s)
$\dot{n}_{CO2,syng}$	Molar flow rate of carbon dioxide in treated syngas (mol/s)
$\dot{n}_{H2,r.g.}$	Molar flow rate of hydrogen in selected reject gases (mol/s)
$\dot{n}_{H2,elec,MeOH}$	Molar flow rate of hydrogen produced by the electrolysis unit (mol/s) for methanol synthesis
$\dot{n}_{H2,elec,BM}$	Molar flow rate of hydrogen produced by the electrolysis unit (mol/s) for biomethanation
$\dot{v}_{BM}$	Normal volume flow rate of biomethane
P_{natgas}	Average market price of conventional natural gas (€/kWh)
PtG	Power-to-gas
PtM	Power-to-methanol
Q_{GB}	Enthalpy difference in the gasification bed
Q_{CB}	Enthalpy difference in the char combustion bed
Q_{loss}	Heat losses to the surroundings
S-t-F	Syngas-to-fuel
SAB	Standalone biomethanation
SM	Stoichiometric modulus
T_{DH}	District heat stream temperature
WGS	Water-gas shift

1 Introduction

The implementation of advanced bioeconomies relies on the efficient conversion of renewable carbon stocks into versatile fuels and chemical feedstocks. Biomass gasification has been identified as a promising technology for the thermochemical conversion of renewable biomass into a synthetic gas mixture (syngas) that can serve as a precursor to produce renewable biofuels and biochemicals [1]. Such products are the result of conversion processes operated downstream of biomass gasification and include commodities such as Fischer-Tropsch products, methanol, dimethyl ether, hydrogen, biodiesel, and biomethane in the form of bio-derived substitute natural gas (bSNG) [2]. Syngas upgrading to bSNG via methanation has attracted much attention in recent years [3], partly because of the versatility of methane as a low-emissions energy carrier that makes it a suitable fuel for the transition to a fully renewable energy system [4]. Methanation processes offer the possibility to be integrated in so-called power-to-gas (PtG) systems. In these systems, water electrolysis, powered by surplus renewable electricity, is used to produce hydrogen, which reacts with carbon dioxide to synthesize grid-quality bSNG [5], either via catalytic [6] or via biological conversion processes [7]. PtG processes offer several opportunities for future energy systems, enabling energy storage and grid stabilization while producing renewable methane [8]. Biomass gasification can thus be integrated with methanation and water electrolysis in PtG systems, with the potential to address fuel-type diversification and storage needs. Integrated biomass gasification and catalytic methanation systems have been widely studied from a modeling and system performance point of view [9], while only few studies so far have addressed the performance of integrated biomass gasification-biomethanation systems [10–12].

Among the products of syngas conversion, methanol is a fundamental platform chemical for the production of a variety of compounds in the contemporary chemical industry, such as formaldehyde, methyl tert-butyl ether, and acetic acid [13] and the production of bio-derived methanol could play an important role in future biorenewable supply chains. Methanol has also been identified as a promising transition fuel and energy carrier to lead the transportation sector towards complete decarbonization [14]. Therefore, the development of biomass-to-methanol technologies and the techno-economic analysis of related full-scale processes have recently attracted considerable attention [15]. An integrated biomass gasification-methanol synthesis (IBGM) scheme comprises biomass gasification to syngas and the subsequent catalytic synthesis of methanol via CO conversion to CO_2 and subsequent hydrogenation (the CAMERE process), or via direct CO_2 hydrogenation. Catalytic methanol synthesis from direct CO_2 hydrogenation can serve as a carbon utilization process [16, 17] that allows the fixation of CO_2 from a variety of sources into a useful product, and it can be integrated into power-to-methanol (PtM) systems, where renewable electricity is exploited to produce electrolytic hydrogen for use in methanol synthesis [18]. When large quantities of renewable hydrogen are available, CO_2 hydrogenation to methanol represents an option for the valorization of renewable carbon derived from other processes via carbon utilization, according to the poly-generation needs of future bioeconomies and the biorefinery concept [19]. Moreover, the conversion of CO_2 and H_2 to methanol through the PtM concept allows overcoming the limitations related to the handling of pure hydrogen, by producing a versatile liquid fuel that is more easily exploitable in the existing distribution infrastructure [20]. Moioli et al. [21] demonstrated that CO_2-to-methanol requires an overall lower energy input per unit mass of fuel produced than CO_2-to-methane, due to the lower stoichiometric hydrogen requirements of methanol synthesis, and that it delivers a higher energy storage efficiency when normalized for electrolysis efficiencies. For this reason, CO_2-to-methanol may represent a better option than CO_2-to-methane when small-scale applications are considered, due to the lower investment required by smaller electrolysis sizes.

Biological methanation (biomethanation) of biogas produced through anaerobic digestion has seen successful lab-scale demonstration [22–24] and pilot projects [25], and its use in PtG schemes has been investigated taking AD as a standalone carbon source [26] or in parallel to hydrothermal liquefaction (HTL) of digestate [27]. For standalone AD, Vo et al. [26] estimated a biomethane minimum selling price (MSP) of 1.43 €/Nm^3, with an electricity cost of 0.1 €/kWh. Kassem et al. [27], instead, estimated a biomethane levelized cost of energy (LCOE) of 10 $/GJ (approx. 0.33 €/$Nm^3$, conversion rate 1 EUR = 1.1 USD), considering an electricity price of 0.05 $/kWh and applying two US carbon pricing mechanisms on the biomethane and the biocrude produced through HTL, namely the Low Carbon Fuel Standard (LCFS) and the Renewable Fuel Standard (RFS). However, none of the two studies evaluated the effect of utilizing the available CO_2 for two distinct product streams with the aid of electrolytic hydrogen.

Biomethanation of syngas has also recently been demonstrated an effective syngas-to-methane technology on the lab scale and shows potential for scale-up [28]. In a previous techno-economic assessment on an integrated biomass gasification-electrolysis-biomethanation (IBGEB) process, we identified a bSNG minimum selling price of 2.68 €/Nm^3 and we indicated that key optimization opportunities rely on lower-pressure operation and better energy integration within the process [11]. As an important advantage over catalytic methanation, syngas biomethanation offers the possibility of low-pressure [22, 23] or atmospheric-pressure [28] operation, with the potential to generate energy savings. However, such advantage can only be exploited if the upstream process train is run at lower pressure, avoiding high-pressure units in the syngas gas conditioning section. In syngas conditioning, impurities such as H_2S and NH_3 need to be removed by a combination of water scrubbing and/or catalytic reactions, and the CO_2:H_2 ratio of the feed gas needs to be lowered to avoid excessive CO_2 concentration in the product SNG, or conversely, to limit the additional hydrogen demand from electrolysis. An alternative to the use of high-pressure catalytic units for desulphurization and water-gas shift (WGS) [29, 30] is the simultaneous removal of CO_2, H_2S and NH_3 from syngas by combined water-methanol scrubbing [30] that can be effective at low pressures when the required reduction in concentration is limited.

Yun et al. [31] recently proposed an alternative concept to the conventional gasification-cleaning-methanation train, illustrating the use of biomass pyrolysis followed by low-temperature steam reforming of bio-oil as a promising strategy for the direct production of biomethane with high carbon conversion efficiency. The improvement of carbon efficiency in biomass-to-biomethane systems can also be addressed through the capture and utilization of carbon streams rejected by the process that could be further exploited on site to produce renewable commodities. Michailos et al. [10] have modeled carbon capture and storage (CCS) by amine scrubbing on a gasification-biomethanation process, indicating that the system could capture 1.42 kg CO_2 per kg bSNG produced, increasing the bSNG minimum selling price (MSP) by 17% compared to a process without CCS. The authors indicated that the examined biomethanation process would only be profitable (NPV = 0) with a price of 39 £/t of CO_2 captured and a penalty emission factor on fossil natural gas of 0.2 t CO_2/MWh. However, alternative carbon utilization options of the recovered carbon stream were not assessed in the study. Michailos et al. [12] also evaluated an integrated concept for a wastewater treatment plant comprising anaerobic digestion (AD), digestate gasification, and CO_2 biomethanation, where AD and PEM electrolysis are the main source of CO_2 and H_2, respectively. In scenarios in which digestate gasification is used for the co-provision of H_2 or a mixture of CO_2 and H_2 to biomethanation, the estimated MSP were 135 £/MWh_{HHV} (approx. 1.65 €/Nm^3; 1 GBP = 1.09 EUR) and 164 £/MWh_{HHV} (approx. 2 €/Nm^3), respectively, with reductions of 32–42% when O_2 valorization, renewable energy incentives, and grid balancing fees are included. However, the co-production of more than one fuel type was not considered in any of the layouts studied.

Further work is thus required in order to assess process integration options that can enhance the feasibility of IBGEB processes, increase their carbon efficiency, and allow for poly-generative systems that valorize waste renewable carbon. The techno-economic modeling of low-pressure biomethanation systems integrated with high-value power-to-X and carbon utilization options is required in order to assess the potential of these processes to improve the large-scale feasibility of biomass-to-biomethane systems.

In this study, we implemented a techno-economic process model to assess two alternative options for the valorization of biomass carbon through the production of bSNG, biomethanol, and district heat. In a base case, we investigated the performance of an integrated biomass gasification-electrolysis-biomethanation (IBGEB) system in which low-pressure syngas conditioning is implemented via water-methanol scrubbing. In an alternative case, we assessed the performance of the same IBGEB process where the carbon stream left unconverted by the process is utilized in catalytic methanol synthesis.

The aim of the study was to verify whether carbon utilization for methanol synthesis can improve the techno-economic performance of an IBGEB process and lower the bSNG minimum selling price. In particular, we implemented a steady-state process model in Aspen® Plus, and for each process, we estimated (1) mass balances, (2) energy balances, and (3) biomethane minimum selling price under different economic scenarios.

2 Materials and methods

2.1 Process description

2.1.1 Standalone biomethanation

In standalone biomethanation (SAB), wet wood pellets are dried and converted to syngas in a 32-MW_{th} dual-fluidized bed steam gasification plant, based on the size and configuration of the GoBiGas plant [30] (Fig. 1). Hot syngas is used to generate steam in a counter-current heat exchanger; it crosses a bag filter for the removal of particles and then transfers to the liquid scrubbing section (Fig. 2).

Particle-free syngas (SYNG-4) is cooled to 25 °C and compressed to 5 bar, before entering a water scrubber (W-SCRUB) for the reduction of NH_3, H_2S, and CO_2 concentration. Rich water (SPWATER) is stripped with air for the removal of the absorbed compounds and is partly recycled to the scrubber, where it is mixed with make-up water. Pre-treated syngas (SYNG-6) passes through a condenser and enters a chilled methanol scrubber (MEOHSCR) for further removal of NH_3, H_2S, and CO_2. Rich methanol is depressurized (H2SSTRIP) and regenerated in a distillation column (CO2STRIP). Regenerated methanol (MEOHREG) is recycled to the scrubber inlet and mixed with fresh solvent.

Downstream of the scrubbing section (Fig. 3), treated syngas is warmed to a thermophilic temperature of 60 °C (SYNG-11); it mixes with an additional hydrogen stream and enters a trickle-bed reactor for syngas bioconversion to biomethane. The produced biogas (BIOG-1), a wet mixture of CH_4, CO_2 and impurities, is dried in a condenser and is then compressed to 10 bar and cooled to 15 °C upstream of a pressure swing adsorption (PSA) unit for biogas purification. Purified bSNG (BIOMTN) is then injected into the gas grid at 70 bar through a multi-stage intercooled compressor (MSCOMP-1). The stoichiometric modulus (SM, Eq. (1)) represents the ratio between H_2, CO, and CO_2 required to achieve full stoichiometric carbon conversion in a biomethanation system [32].

$$SM = \frac{\dot{n}_{H_2} + \dot{n}_{CO}}{\dot{n}_{CO_2} + \dot{n}_{CO}} = 4 \tag{1}$$

However, in order to limit the size of the electrolysis plant required, in this study, an alkaline electrolyzer supplies additional hydrogen to satisfy only a H_2:CO_2 ratio of 4, thus leaving part of syngas carbon unconverted. The oxygen produced by the electrolysis plant is used for in-plant combustion of reject gases (CMBSTR-2, below).

Figure 4 and 5 display a representation of the energy recovery train. The mixture of reject gases (TAILS-0) is combusted at 920 °C and combustion heat is recovered by producing steam (STM-F-2) that transfers heat to the reboiler of the methanol regeneration column (heat stream Q-8, Fig. 2), is used to warm syngas (HX-9, Fig. 3), and finally mixes with other steam lines destined to district heat provision (not displayed). The off-gases from the reject gas combustor (CMBSTR-2) and from the char combustion bed (CMBSTR-1) are cooled to 220 °C while transferring heat to a 50-bar steam line (STM-B-1, Fig. 5), which is subsequently expanded in a series of two turbines, first through a 35-bar pressure decrease, and then to a final pressure of 3 bar. The cooled off-gases at 220 °C (FLUE-6) enter the biomass dryer before being ejected to the atmosphere. Further heat is recovered from the low-temperature steam exiting the turbine cycle

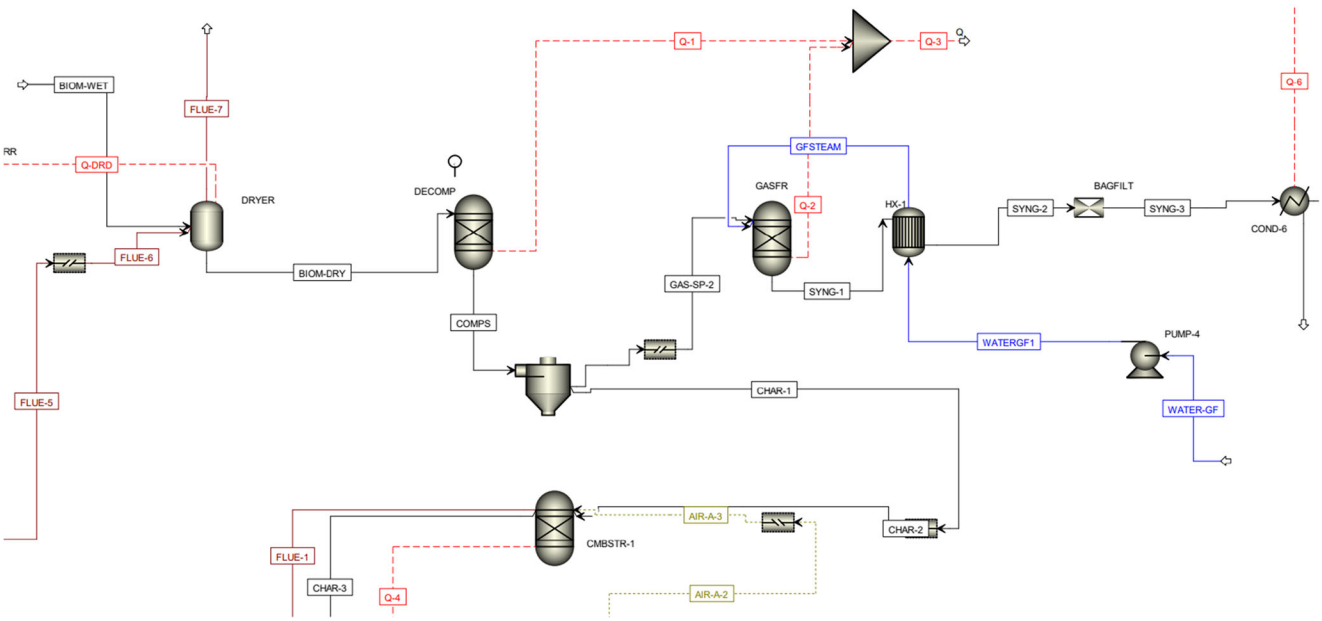

Fig. 1 Biomass drying, dual fluidized bed steam gasification, syngas cooling, particles, and moisture removal

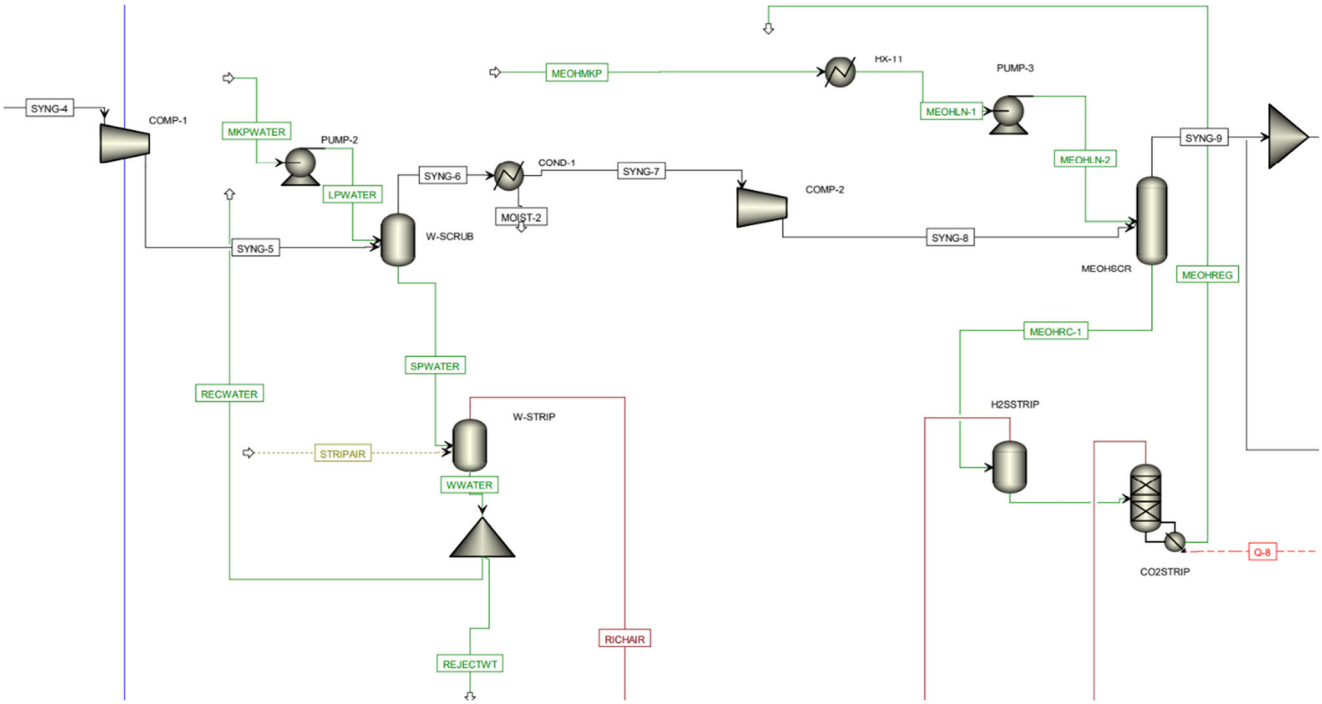

Fig. 2 Syngas water-methanol liquid scrubbing and related solvent regeneration sections

(STM-B-6) and transferred first to incoming steam (through HX-3) and secondly to the biomass dryer.

2.1.2 Integrated biomethanol-biomethane

In addition to the gasification, syngas conditioning, and biomethanation sections described above, in the integrated biomethanol-biomethane (IBB) process, the unconverted carbon stream rejected in biogas purification is exploited in catalytic biomethanol synthesis (Fig. 7) on a $Cu/ZnO/Al_2O_3$ catalyst [21]. Tail-gases from PSA biogas treatment are combusted (CMBSTR-3) to heat a steam line (STM-I) that supplies heat to the methanol distillation train and is then sent to district heat provision (not displayed). A mix of plant reject gases is combusted in a second combustor (CMBSTR-2) (Fig. 6), to produce another 50-bar steam line (STM-F) for expansion in the turbine cycle. A third steam line is produced by cooling the off-gases from the reject gas combustor and the

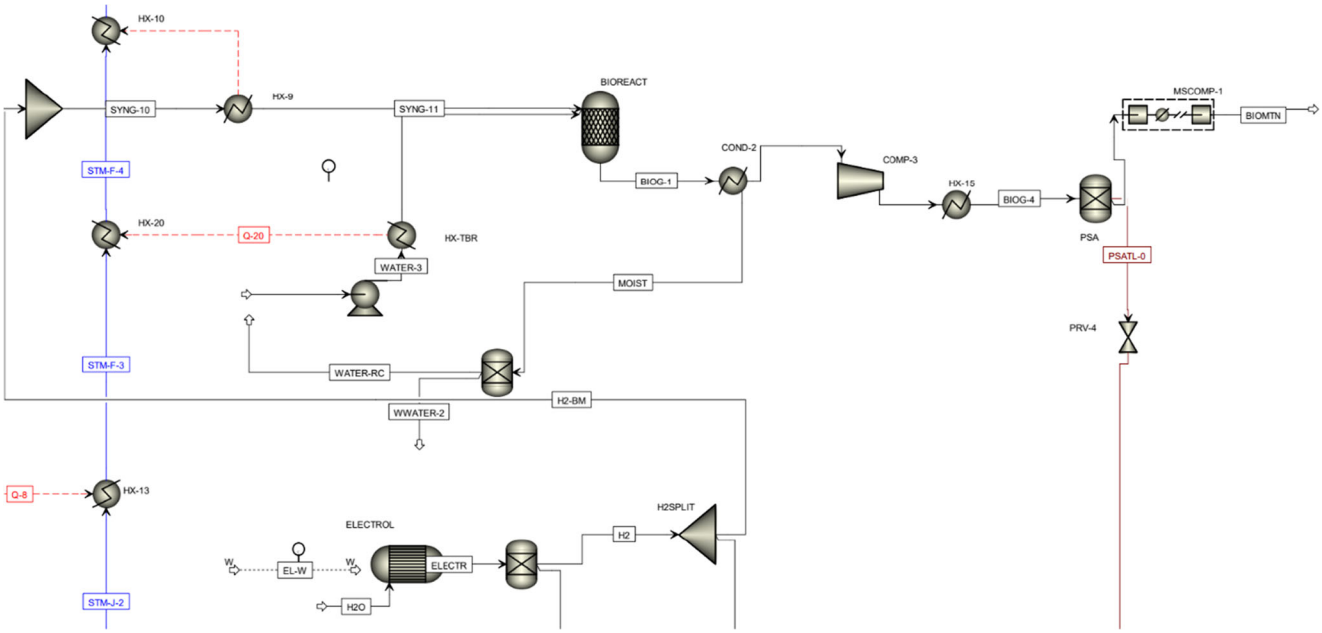

Fig. 3 Syngas biomethanation, biogas purification, and electrolysis

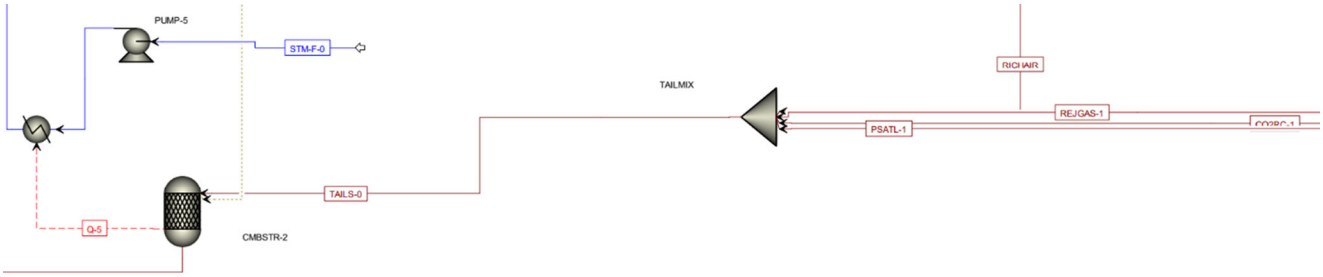

Fig. 4 Combustion of rejected plant gases for energy recovery (SAB process)

char combustion bed. The oxidized off-gases from PSA tail gas combustion (CU-1) transfer to the methanol synthesis section and mix with additional hydrogen from the electrolysis plant. The feed mixture is cooled and compressed to the reaction pressure (50 bar) in a multi-stage compressor. The reaction heat generated by CO_2 hydrogenation is used to pre-heat STM-I, while further cooling of the reaction products transfers heat to a further steam line (STM-J) for use in the biomethanation section.

The reaction products are cooled to 10 °C and separated in a first flash drum. The liquid phase obtained is cooled and expanded in a second flash drum (10 °C, 1.2 bar). The gas-

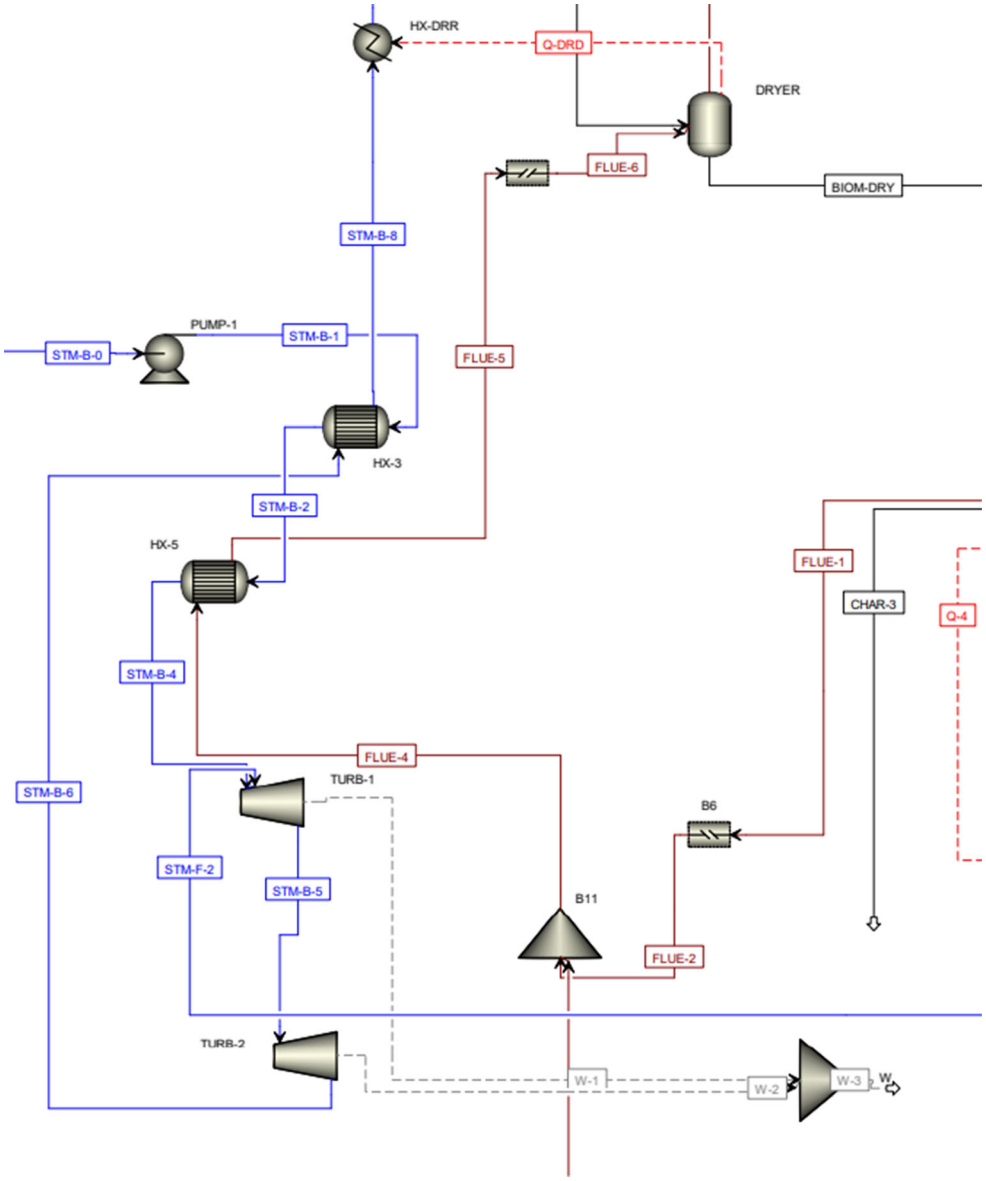

Fig. 5 Fuel gas cooling and steam cycle

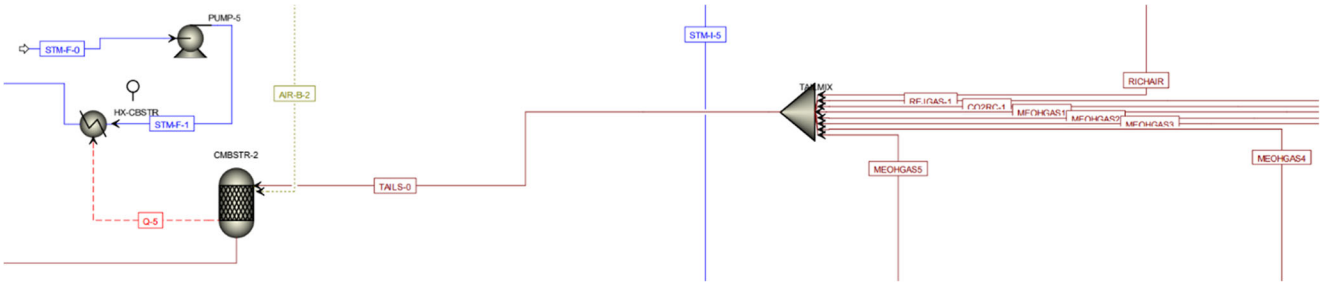

Fig. 6 Combustion of rejected plant gases for energy recovery (IBB process)

phase streams (MEOH-G-1, MEOH-G-2) are sent to combustion for energy recovery. Raw methanol (MEOH-4) is purified in a three-step distillation train, with intermediate flash gas separation and condensation units to achieve a > 99% purity in the top product of the third column. The columns reboilers exchange heat with the hot steam line STM-I, while heat is recovered from the largest wastewater stream (MEOH-5).

2.2 Process modeling methods

All physical, chemical, and thermal process modeling was carried out in Aspen® Plus v.10, while the evaluation of economic scenarios for the two processes was carried out in Excel®. The following sections provide details on the modeling methods.

2.2.1 Biomass steam gasification

In the simulation of complex integrated flowsheets, biomass steam gasification has frequently been modeled by separating the pyrolysis-gasification process and the char combustion process. Under this approach, a mass and heat balance is calculated around the pyrolysis-gasification zone, the unconverted char is transferred to the combustion zone, and char combustion heat is set equivalent to the enthalpy requirements of the pyrolysis-gasification process, allowing for a fraction of heat loss [33, 34]. Some authors have simulated the pyrolysis-gasification process (gasification bed) as a single-step gas formation process, either by using experimental data to reconcile a thermodynamic model [35, 36] or by directly implementing empirical correlations [37]. Another approach consists in subdividing the gasification bed into a biomass decomposition step and a gas formation step [10]. The DFB steam gasification process in this study was modeled according to a three-step methodology that simulates biomass decomposition, permanent gas and tar formation and char combustion. A constant biomass composition is adopted according to the experimental data reported by Alamia et al. [34]. Biomass enthalpy is estimated through the HCJ1Boje method and biomass density through the DCOALIGT method [38] that can be applied to non-conventional solid streams in Aspen Plus and RK-Aspen was selected as the thermodynamic property method used in

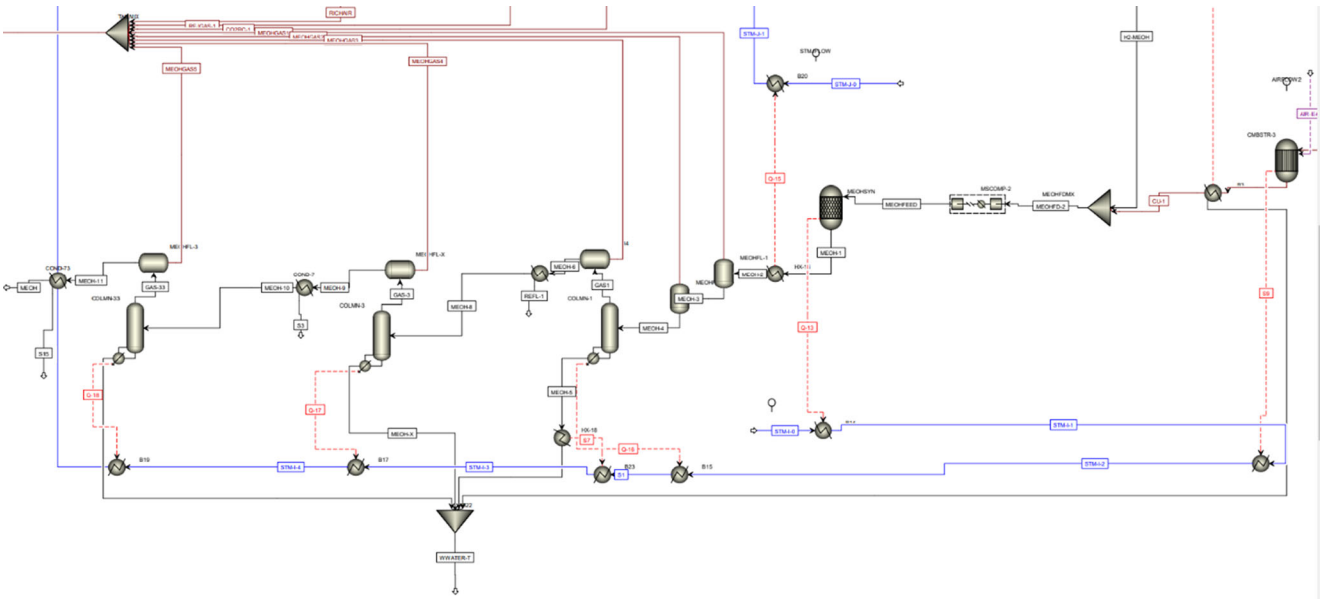

Fig. 7 Catalytic methanol synthesis and purification

the gasification section [37, 38]. Biomass moisture content is represented as a separate H_2O stream in the mixed composition of biomass, to enable vapor-liquid flash calculations (Aspen Flash2) in the drying process. Two RYield units are used in Aspen Plus to first decompose biomass into H_2, CO, CO_2, CH_4, and C (DECOMP), according to its elemental composition, and secondly to yield the gas composition reported for the GoBiGas plant [30] (GASFR). Tar compounds were restricted to four species representing one tar class each (phenol, class 2; toluene, class 3; naphthalene, class 4; coronene, class 5). Their relative concentration and yield was adapted from Zhang and Pang [39]. The concentration of H_2S was estimated from the mass yield reported for the GoBiGas plant [34]; NH_3 concentration was estimated from N elemental balance assuming 100% conversion to NH_3, while the Cl biomass concentration applied (0.006%) was considered sufficiently small to neglect any HCl formation in this study. Char production corresponded to a mass rate of 0.186 kg_{char}/kg_{DB} [34] and its composition was modeled as pure C (CISOLID class in Aspen Plus). Char produced in the gasification bed is separated from the products of biomass decomposition (DECOMP) with a Sep block and it is fully combusted in air at 850 °C (CMBSTR-1, RGibbs), according to a restricted thermodynamic equilibrium approach in RGibbs, where only CO_2, O_2, and C were set as possible products.

The model described allowed reaching a deviation of 1% on C atomic balance across the gasifier. Gas moisture content was then estimated by closing the H balance.

In a DFB gasifier, the combustion heat generated in the char bed (CMBSTR-1, Fig. 1) is transferred to the gasification bed through a solid heat transfer medium [40]. Char combustion heat (Q-4) can thus be considered equal to the enthalpy requirements of the gasification bed, while accounting for heat losses (Eq. (2)), according to a DFB concept [34, 35, 37].

$$Q_{GB} = Q_1 + Q_2 = Q_{CB} - Q_{loss} = Q_4 \quad (2)$$

In this model, the enthalpy balance around the gasification bed was calculated in Aspen Plus as the algebraic sum (heat stream Q-3) of the enthalpy balances of the biomass decomposition (DECOMP, heat stream Q-1) and permanent gas formation (GASFR, heat stream Q-2) at isothermal conditions (850 °C, 1 atm). Char combustion was also calculated at isothermal conditions (920 °C, 1 atm, heat stream Q-4). The difference between heat streams Q-4 and Q-3 can be assumed to cover heat losses and is not articulated any further in this study. The DFB heat balance could thus be defined as in Eq. (3).

$$Q_4 = Q_1 + Q_2 + Q_{loss} = Q_3 + Q_{loss} \quad (3)$$

2.2.2 Syngas conditioning and solvents regeneration

At the gasifier outlet, syngas is cooled below 200 °C while bringing gasification steam to a temperature setpoint of 350 °C in HX-1. Subsequently, a bag filter with a 100% particle removal efficiency is simulated through a simple pressure reduction device (Valve). The water scrubber is simulated as a single-stage adiabatic flash (W-SCRUB, Flash2), while the methanol scrubbing section is modeled through a simplified adaptation of the Rectisol® process for syngas treatment [41]. The scrubbing tower is simulated by an adiabatic absorber (MEOHSCR, RadFrac) with five equilibrium stages and a chilled methanol (− 60 ° C) inflow rate of 2 kg/s (solvent-to-feed rate of approximately 1.25 kg_{MeOH}/kg_{syngas}). Stripping of rich water takes place in a single-stage adiabatic flash column (W-STRIP, Flash2). Methanol is first depressurized in a single-stage flash drum (H2SSTRIP, Flash2) at near-ambient conditions and it is then regenerated in a 10-stage distillation column (CO2STRIP, RadFrac) without condenser. The regenerated methanol stream leaves the column reboiler as a liquid at boiling point. Methanol cooling is represented through a heater block (− 60 °C) on the incoming lean methanol stream that enters MEOHSCR. Table 1 provides a summary of the specified operating conditions for the vapor-liquid equilibrium units. All separation processes within the syngas conditioning and solvents regeneration section are simulated through vapor-liquid equilibrium (VLE) [42] according to the ELECNRTL model state equation, as recommended for acid gas absorption [43] and as previously used in the simulation of syngas scrubbing [37, 44].

2.2.3 Biomethanation and bSNG grid injection

Biomethanation of syngas takes place in a trickle-bed bioreactor, a reactor configuration that has been demonstrated to achieve high H_2 conversion on the lab scale and shows potential for scale-up [28]. The biomethanation process is simulated through a stoichiometric reactor (BIOREACT, RStoich), where syngas is converted to biogas according to Reaction 1 and Reaction 2, at a 95% once-through conversion efficiency on hydrogen and carbon monoxide, respectively, according to the performance of trickle-bed reactors reported by Asimakopoulos et al. [28].

Reaction 1

$$CO_2 + 4H_2 \rightarrow CH_4 + 2\,H_2O$$

Reaction 2

$$4CO + 2H_2O \rightarrow CH_4 + 3\,CO_2$$

Liquid recirculation to the reactor is simulated through a pump, while nutrient provision modeling is not part of this

Table 1 Summary of specified operating conditions for vapor-liquid separation units in the syngas conditioning section

Unit process	Unit ID	Block type	Specified temperature °C	Top-stage pressure bar	Number of equilibrium stages -	Pressure drop bar	Specified gas inflow rate kg/s	Specified liquid inflow rate kg/s	Column convergence Aspen specification -
Water scrubber	W-SCRUB	Flash2	Adiabatic	5	1	0.6	-	100.0	-
Methanol scrubber	MEOHSCR	RadFrac	Adiabatic	5	4	0.6	-	2.0	-
Water stripper	W-STRIP	Flash2	Adiabatic	1.01	1	Isobaric	2.2	-	-
Methanol flash	H2SSTRIP	Flash2	20	1.2	1	Isobaric	-	-	-
Methanol regenerator	CO2STRIP	RadFrac	Adiabatic	1.2	10	0.6	-	-	Bottoms-to-feed ratio: 0.97 mol/mol

study, although in a typical trickle-bed reactor, the microbial community is fed with a solution containing nitrogen, phosphorus, potassium, other minor nutrients, and pH buffer salts [22, 23, 28, 45, 46].

The biogas mixture at the bioreactor outlet is purified by means of a pressure swing adsorption (PSA) unit, modeled as a simple separator (Sep) operating at 10 bar with specified constant separation efficiencies for the selected compounds reported in Table 2. The pure-stream side recovery rate of all other compounds was assumed to be zero. A pressure reduction valve (Valve) is used to depressurize the wasted stream to atmospheric pressure, according to a typical depressurization-wasting cycle in a PSA system.

Gas compression for grid injection of the purified stream is modeled through an inter-cooled multi-stage compressor (MComp) with three constant 18-bar pressure increase steps and a final 16-bar stage.

2.2.4 Catalytic methanol synthesis and purification

Although the CAMERE process can deliver higher carbon conversion rates [47], in this study, direct CO_2 hydrogenation (reaction 3) is selected in order to minimize additional process complexity.

Reaction 3

$$CO_{2(g)} + 3H_{2(g)} \leftrightarrow CH_3OH_{(l)} + H_2O_{(l)}$$

The efficiency of direct CO_2 hydrogenation is limited by low per-pass conversion rates [48]; therefore, configurations with multiple reactors in series (cascade) or intensive recycle loops are required in order to improve the overall carbon conversion rates achieved [21, 49, 50]. Direct CO_2 hydrogenation processes have been previously been modeled through kinetic models with multi-step recycle loops [51–53]. In this study, a simplified representation of methanol synthesis is obtained as follows. A cascade system with internal recycle is simulated through a single isothermal reactor (MEOHSYN, RStoich, Table 3). A global CO_2 conversion rate of 65% is applied to the reactor boundaries, according to the overall CO_2

Table 2 Specified constant separation efficiencies for the selected compounds

Selected compound	Recovery rate (% mol/mol)
CH_4	97
H_2	10
CO	5
CO_2	2.5
H_2S	1
NH_3	1

Table 3 Summary of specified process operating conditions in methanol synthesis and purification

Unit process description	Unit ID	Block type	Temperature °C	Pressure bar
Catalytic methanol reactor	MEOHSYN	RStoich	250	50
Flash tanks	MEOHFL-1	Flash2	Adiabatic	50
	MEOHFL-2		4	1.2
	MEOHFL-3		55	1.2
	MEOHFL-4		55	1.2
	MEOHFL-4		65	1.2
Heat exchangers and condensers	HX-16	Heater	25	Isobaric
	COND-3		4	1.2
	COND-4		2	1.2
	COND-5		2	1.2
	COND-6		2	1.2

conversion estimated by Moioli et al. [21] for a cascade configuration with optimal energy storage efficiency. Unit processes internal to the cascade configuration and recycle loops are not articulated further in this study. Table 3 provides a summary of the operating specifications applied to the simulation of methanol synthesis. The RK-Soave thermodynamic property method was used to simulate methanol synthesis and purification [51, 53, 54].

Methanol purification is carried out via the three-step distillation process previously described (Fig. 7) and simulated by three RadFrac blocks, with specified top-stage pressures and bottoms-to-feed molar ratios (Table 4). The operating conditions of the intermediate vapor-liquid flash separation and heat exchange equipment are detailed in Table 3.

2.2.5 Alkaline electrolysis

Alkaline electrolysis has recently seen wide application in PtG projects [25] as well as the development of the first 10-MW plant worldwide in Japan [55, 56]. Due to its mature technological development and to its durability and cost-competitiveness [57–59], alkaline electrolysis was selected as the power-to-hydrogen technology in this study. A constant efficiency of 4.4 kWh per Nm^3 of H_2 output [59] was assumed and total hydrogen flow rate was calculated by a calculator block in Aspen Plus to satisfy a stoichiometric flow for Reaction 1 and Reaction 3.

2.2.6 Energy recovery via combined cycle

Combustion of the mixed gases takes place in an isothermal combustor (COMBSTR-2, RStoich) to generate steam as previously described. The first steam turbine decreases the steam pressure by 35 bar while the second turbine has a specified outlet pressure of 3 bar. The resultant low-pressure steam is used to pre-heat water and supply heat to the dryer, by lowering steam enthalpy (heater blocks) by an amount equivalent to the heat duty required in each unit process attached, while avoiding temperature crossovers. Heat transfer between these units is simulated via heater blocks and heat exchangers' feasibility is not articulated further. The two low-temperature steam lines are finally combined and are available for further low-temperature heat provision in a district heating system. The available heat to be exploited in district heating is estimated by cooling steam to 20 °C in a heater block (HX-DH).

2.2.7 Efficiency indicators

Thermal efficiency considers the fraction of biomass LHV stored as fuel LHV or exportable heat, neglecting the additional work inputs (Eq. (4)).

$$\eta_{th} = \frac{\sum_{i=1}^{n} \dot{m}_{prod,i} \times LHV_{prod,i} + \sum_{i=1}^{n} Q_i}{\dot{m}_{db} \times LHV_{biom}} \quad (4)$$

Table 4 Summary of methanol distillation columns specifications

Unit process description	ID	Top-stage pressure bar	Number of equilibrium stages -	Bottoms-to-feed ratio mol/mol
Distillation columns	COLMN-1	1.2	10	0.41
	COLMN-2	1.2	10	0.35
	COLMN-3	1.2	10	0.05

Plant efficiency (Eq (5)) considers the total LHV stored in fuels and exportable heat in relation to the total energy input into the plant, inclusive of biomass LHV and work.

$$\eta_{plant} = \frac{\sum_{i=1}^{n} \dot{m}_{prod,i} \times LHV_{prod,i} + \sum_{i=1}^{n} Q_i}{\dot{m}_{db} \times LHV_{biom} + \sum_{i=1}^{n} W_i} \quad (5)$$

Additional information on turbomachinery efficiency, heat exchangers, and utilities usage is reported in Supplementary Material.

2.3 Economic assessment

2.3.1 Capital and operating costs

Purchased equipment costs were estimated through a factorial method by using base equipment sizes, base costs, and exponential factors retrieved from the literature (Table 5). The total heat transfer area required by the heat exchangers network in the plant was estimated through a preliminary exchanger sizing automatically estimated by the Aspen Economic Analyzer. All other equipment sizes in Table 5 could be retrieved from the plant mass and energy balance. Indirect capital costs were also estimated through the factors on direct costs indicated by Albrecht et al. [64] (Supplementary Material) and the total capital investment (TCI) was estimated according to Eq. (7).

$$C = C_0 \left(\frac{S}{S_0}\right)^f \quad (6)$$

C, actual cost; C_0, base cost; S, actual plant size; S_0, base plant size; f, exponential factor.

$$TCI = FCI + WC = (PEC + DC + IC + AE) + WC \quad (7)$$

TCI, total capital investment; FCI, fixed capital investment; WC, working capital; PEC, purchased equipment cost; DC, direct capital cost; IC, indirect capital cost; AE, additional expenses.

Direct operating costs were calculated from the mass and energy balances obtained from the process model applying the cost rates in Table 6, while labor and indirect operating costs were estimated following the factors indicated by Albrecht et al. [64]. In particular, it was assumed that the electrolyzer works constantly at full load and that the plant operator can obtain a long-term contract in the wholesale electricity market for a fixed rate of 35 €/MWh on power-to-gas electricity.

2.3.2 Minimum selling price estimation

The minimum selling price of biomethane is defined as the biomethane price that makes the project net present value (NPV) equal to zero at a given internal rate of return (IRR), according to Eq. (8).

$$NPV = \sum_{i=1}^{n} \frac{CF_n}{(1 + IRR)^n} = 0 \quad (8)$$

By annualizing the repayment of total capital cost through an annualized capital cost term (ACC) (Eq. (9)) [65], yearly cash flow can be defined as in Eq. (10) and bSNG MSP can be calculated as in Eq. (11), applying the parameters reported in Table 7.

$$ACC = FCI\left(\frac{I(1+I)^n}{(1+I)^n - 1} + I(WCF)\right) \quad (9)$$

$$CF = \left(MSP_{bSNG} \times \dot{v}_{bSNG} + SR{-}OPEX\right)(1{-}t){-}ACC + DEP \times t \quad (10)$$

$$MSP_{bSNG} = \left(OPEX{-}\left(\dot{Q}_{DH} \times P_{DH} + \dot{m}_{MeOH} \times P_{MeOH}\right) + \frac{ACC + DEP \times T}{1{-}T}\right)\frac{1}{\dot{v}_{BM}} \quad (11)$$

Consequently, the difference between bSNG MSP and a base market price for a common alternative energy commodity, such as natural gas, can be estimated as in Eq. (12). Such price gap corresponds to the cost of achieving grid gas renewability through biomass-to-biomethane technologies.

$$P_g = MSP_{bSNG}{-}P_{natgas} \quad (12)$$

2.3.3 Sensitivity analysis on major direct OPEX assumptions

It was previously demonstrated that biomass and surplus electricity cost have a strong impact on the MSP of bSNG-produced biomass-to-biomethane processes [10, 11]. Consequently, these OPEX sources, as well as the selling price of biomethanol as a side product in IBB, are expected

Table 5 Summary of purchased equipment cost estimates

	S_0	S	Unit	C_0 (M€)	Year	f	C (M€)	Reference
Gasification island								
Gasifier	32	33.30	MW_{th}	11.00	2011	0.8	11.36	[30]
Biomass storage, preparation, feeding to atmospheric pressure	64.6	7.09	t_{wet}/h	1.83	2000	0.77	0.37	[60]
Air drier	0	16.42	0	0.00	2003	0	0.00	[60]
Cleaning section								
Fabric filter	15.6	4.85	m^3/s	0.06	2002	0.77	0.03	[60]
Water scrubber	12.1	0.02	m^3/s	2.70	2002	0.7	0.03	[60]
Water stripper	24,123	380.21	kmol/h	3.60	2009	0.7	0.22	[61]
Methanol scrubber	6021.1	215.95	kmol/h	8.81	2007	0.63	1.20	[62]
CO_2 desorption	6021.1	215.95	kmol/h	2.10	2007	0.63	0.29	[62]
Methanol regeneration column	6021.1	215.95	kmol/h	1.08	2007	0.67	0.13	[62]
Biomethanation section								
Bioreactor	5	15.68	MW_{LHV}	2.46	2016	0.6	4.89	[26]
PSA	1	1582.42	Nm^3/h	0.00	2018	0.7	0.78	[63]
Biomethanol synthesis and purification								
Catalytic reactor	5000	226.38	t/d	61.60	2005	0.67	7.74	[47]
Distillation system	5292	226.38	t/d	14.40	2008	0.67	1.74	[47]
Steam cycle - energy recovery								
Combustor	20	7.84	MW_{LHV}	1.97	2014	0.83	0.91	[64]
Turbine cycle	25	1.28	MW_{output}	8.47	2014	0.7	1.06	[64]
Electrolysis								
Electrolyzer	1	24.47	$MW_{installed}$	0.64	2014	1	15.66	[64]
Secondary equipment								
Compressors	413	2932.16	kW_{input}	0.49	2014	0.68	1.86	[64]
Pumps	10	0.03	m^3/s	0.10	2014	0.36	0.01	
Heat exchangers	1000	2596.24	m^2	0.26	2014	1	0.68	
Refrigeration system	500	1149.28	kW_{input}	1.06	2014	0.68	1.87	

to show an important impact on bSNG price gap (Eq. (12)). Therefore, the effect of their variation from the base-case values used in the main process simulations needs to be assessed. For these reasons, a two-parameter sensitivity analysis was carried out on bSNG price gap, by assessing the variation of surplus (PtG) electricity cost and biomass cost for the SAB process, and the variation of PtG electricity cost and biomethanol selling price for the IBB process at a base-case biomass cost of 100 €/t_{dry} (Table 8). An average market price of 0.03 €/kWh for grid natural gas was employed in the renewability cost estimation, based on EU28 statistics [70].

Table 6 Summary of main direct operating cost items

Item	Cost (€)	Unit
Labor	24.00	man-hour
Biomass	100.00	t dry
Electricity	90.00	MWh
Power-to-gas electricity	35.00	MWh
Water	2.00	m^3
Catalyst	56.80	m^3 MeOH output
Wastewater management	2.50	m^3

Table 7 Summary of project information

Item	Symbol	Value	Unit
Project lifetime	n	15	Years
Interest rate	I	10%	-
Tax rate	t	35%	-
Biomethanol selling price[a]	P_{MeOH}	275	€/t
District heat selling price[b]	P_{DH}	0.07	€/kWh

[a] Price published by a commercial operator for fossil methanol for the European market [66]. No renewable energy price incentives were assumed

[b] Typical average price for residential district heat for small consumers in the Northern Italian region [67–69]

Table 8 Summary of parameter variations in the sensitivity analysis on OPEX assumptions

Parameter	Symbol	Unit	Lower bound	Base case	Upper bound	Parameter status	
						SAB	IBB
PtG electricity cost	C_{PtG}	€/MWh	0 (− 100%)	35	105 (+ 200%)	Variable	Variable
Biomass cost	C_{biom}	€/t_{dry}	0 (− 100%)	100	200 (+ 100%)	Variable	Constant at base case
Biomethanol selling price	P_{bMeOH}	€/t	0 (− 100%)	275	619 (+ 125%)	Absent	Variable

3 Results

3.1 Process mass and energy balance

Table 9 and Table 10 report a summary of selected process streams for the SAB and IBB processes, respectively.

As shown in Table 11, the standalone biomethane (SAB) process can produce 37,978 Nm^3/day of grid-injected biomethane, with a volumetric yield on biomass of 0.24 Nm^3_{BM}/kg_{DB} and a corresponding plant efficiency of 47% on biomass thermal input (Table 12). The SAB process delivers 6.3 MW of district heat available at 100 °C (Fig. 8). In addition to the same biomethane output, the integrated biomethane-biomethanol (IBB) process can produce 10 t/day of biomethanol with a 99% purity at a mass yield of 0.09 kg_{MEOH}/kg_{DB}. As a result of heat integration, the IBB process also delivers 11.9 MW of district heat (Fig. 9).

Table 11 also displays the biomass-to-fuel (B-t-F) and syngas-to-fuel (S-t-F) carbon efficiency of the two alternatives, indicating that IBB brings substantial advantages in terms of carbon efficiency, storing an additional carbon stream equivalent to 7281 t/y of CO_2 as pure methanol. Consequently, the global B-t-F efficiency of the IBB process is 27% higher than in SAB, demonstrating that despite the increase in plant size and complexity, bSNG production with carbon utilization could play an important role as a carbon management strategy. Equally, S-t-F efficiency is higher in IBB (42%) than in SAB (33%). The greatest carbon loss in SAB is related to the absence of CO_2 utilization and the complete rejection of off gases. The IBB scenario still presents major losses other than flue gases from combustion. These include especially rejected carbon streams in methanol purification, such as wastewater, with an overall methanol recovery of 82% across the distillation train.

The estimated biomethanol yield on CO_2 is 0.47 kg_{MeOH}/kg_{CO2} upstream of distillation and 0.31 kg_{MeOH}/kg_{CO2} considering pure product output, which is similar to the yield estimated by Crivellari et al. [52] (0.36 kg_{MeOH}/kg_{CO2}) in the thermoeconomic modeling of methanol production from surplus wind energy. The estimated yield, however, is lower than reported in most previous studies on direct CO_2 hydrogenation to methanol, probably due to the absence of intensive recycling loops in study, where combustion of unconverted gases is preferred over complex recycling infrastructure. In particular, the estimated yield is 53% lower than estimated by Van-Dal and Bouallou [51] and by

Table 9 Summary of selected process streams for the SAB process

Stream ID									
Parameter	Unit	SYNG-1	MEOHREG	CO2RC-1	SYNG-11	BIOG-2	BIOMTN	TAILS-0	FLUE-7
Temperature	C	815.0	80.0	61.9	60.0	5.0	35.0	21.8	120.0
Pressure	bar	1.0	1.8	1.2	1.0	4.0	79.6	1.0	1.0
Total mole flow	kmol/day	9125.1	5214.3	161.3	7207.4	2929.5	1726.1	8717.3	10,847.0
Mole fractions		5.07	0.00	0.26	5.69	58.99	97.11	1.20	0.00
CH_4		19.59	0.00	0.00	62.48	7.69	1.30	2.33	0.00
H_2		11.95	0.00	0.07	14.53	1.79	0.15	1.07	0.00
CO		18.02	0.00	20.22	15.62	27.39	1.16	14.92	25.68
CO_2	%	41.36	0.01	0.00	0.00	0.00	0.01	2.18	20.07
H_2O		0.00	0.00	0.00	0.00	0.00	0.00	58.47	46.99
C_2H_2		0.07	0.00	0.37	0.05	0.12	0.00	0.07	0.00
C_2H_4		1.53	0.00	0.93	1.39	3.41	0.00	1.60	0.00
CH_3OH		0.00	99.54	75.44	0.06	0.16	0.27	2.27	0.00
H_2S	ppm_{mol}	106.4	0.0	1133.7	17.0	41.9	0.7	111.2	0.0
NH_3		567.3	0.0	22,834.5	1.4	3.4	0.1	591.7	0.0

Table 10 Summary of selected process streams for the IBB process

Stream ID													
Parameter	Unit	SYNG-1	MEOHREG	CO2RC-1	SYNG-11	MEOHFEED	BIOG-2	BIOMTN	MEOH-1	MEOH	TAILS-0	WWATER-T	FLUE-7
Temperature	C	815.0	80.0	61.9	60.0	250.0	5.0	35.0	250.0	4.0	21.9	31.3	120.0
Pressure	bar	1.0	1.8	1.2	1.0	50.0	4.0	79.6	47.0	1.2	1.0	1.0	1.0
Total mole flow	kmol/day	9125.1	5214.3	161.3	7207.5	4498.7	2929.5	1726.3	3068.6	457.3	9169.3	1312.7	12,250.4
Mole fractions													
CH_4		5.07	0.00	0.26	5.69	0.00	58.99	97.11	0.00	0.00	0.58	0.00	0.00
H_2		19.59	0.00	0.00	62.48	74.50	7.69	1.30	39.32	0.00	13.16	0.00	0.00
CO		11.95	0.00	0.07	14.53	0.00	1.79	0.15	0.00	0.00	0.47	0.00	0.00
CO_2		18.02	0.00	20.22	15.62	24.83	27.39	1.16	13.11	0.12	10.03	0.00	21.58
H_2O	%	41.36	0.01	0.00	0.00	0.01	0.00	0.01	23.31	0.84	2.09	81.24	23.41
N_2		0.00	0.00	0.00	0.00	0.01	0.00	0.00	0.01	0.00	55.59	0.00	41.61
C_2H_2		0.07	0.00	0.37	0.05	0.00	0.12	0.00	0.00	0.00	0.03	0.00	0.00
C_2H_4		1.53	0.00	0.93	1.39	0.00	3.41	0.00	0.00	0.00	0.43	0.00	0.00
CH_3OH		0.00	99.54	75.44	0.06	0.00	0.16	0.27	23.30	99.03	2.33	18.76	0.00
H_2S	ppm_{mol}	106.4	0.0	1133.7	17.0	0.0	41.9	0.7	0.0	0.0	92.4	0.0	0.0
NH_3		567.3	0.0	22,834.5	1.4	0.0	3.4	0.1	0.0	0.0	561.4	0.0	0.0

Table 11 Summary of process mass balance and efficiency indicators

Indicator	Unit	Process	
		SAB	IBB
Product output			
Biomethane	Nm^3/day	37,978	37,975
Biomethanol	t/day	-	10
Product yield			
Biomethane	Nm^3/kg_{DB}	0.24	0.24
Biomethanol	kg/kg_{DB}	-	0.09
Carbon efficiency			
Biomass-to-fuel	mol C_{fuel}/mol C_{db}	26%	33%
Syngas-to-fuel	mol C_{fuel}/mol C_{syng}	33%	41%
Carbon dioxide utilized	t/year	-	7281
bSNG specific work input			
Total	kWh_{el}/Nm^3_{bSNG}	7.65	17.01
Before electrolysis	kWh_{el}/Nm^3_{bSNG}	0.73	1.54

Alsayegh [71] (0.67 kg_{MeOH}/kg_{CO2}) for a direct CO_2 hydrogenation process through a kinetic model in Aspen Plus. Pérez-Fortes et al. [72] estimated a 0.68 kg_{MeOH}/kg_{CO2} from an adaptation of the same process, while Anicic et al. [47] estimated a 0.65 kg_{MeOH}/kg_{CO2} yield for a CO_2-to-methanol process modeled with two reactors in series and gas recycle at a constant single-pass conversion efficiency of 21%.

Figure 8 and 9 display a summary of the main energy streams in the two processes, indicating that the plant thermal efficiency in the IBB option is 26% higher than in SAB (82.9 vs. 66.1%) (Table 12). However, the global plant efficiencies are practically similar (50.6% and 51.7%), indicating that the additional energy stream required by intensive hydrogen supply in IBB is stored at a comparable rate with the SAB process, although a larger share of total energy input is recovered as lower-quality district heat in IBB, rather than as storable fuel. Only 24.9% and 5.8% of total energy input is stored as methane and methanol, respectively, in the IBB process. This indicates that the lower hydrogen conversion efficiency in methanol synthesis, compared with methane biosynthesis, limits the overall efficiency of the integrated process from an energy efficiency point of view. However, a sole energetic evaluation of the two systems does not highlight the benefits of producing methanol as a chemical feedstock for local supply chains and a chemical exergy assessment would provide more representative comparisons. The net exportable thermal energy stream generated by both plants is district heat available at 100 °C (6.3 and 11.9 MW for SAB and IBB, respectively). The combined steam cycle also yields 0.98 MW and 1.28 MW of electricity, which serves for parasitic consumption in both scenarios.

The two processes require no direct thermal inputs other than biomass, while electrical consumption is largely dominated by electrolysis in both cases (90% in SAB and 91% in IBB), as a result of the absence of any WGS unit. The resulting specific energy input for bSNG is 7.65 kWh/Nm^3_{bSNG} for SAB, compared to 2.3 kWh/Nm^3_{bSNG} for an IBGEB process with WGS [11]. This indicates that entirely avoiding catalytic WGS largely increases electrolytic hydrogen demand and consequently the specific energy demand of the renewable biomethane produced. Neglecting electrolysis, however, the specific work input in this study is 0.73 kWh/Nm^3_{bSNG}, compared to approximately 2 kWh/Nm^3_{bSNG} in our previous study [11] and approximately 1.5 kWh/Nm^3_{bSNG} for an integrated gasification-biomethanation process without electrolysis [10]. The specific energy input for the IBB process is 17 kWh/Nm^3, although this includes the production of methanol. Gas compression includes bSNG injection into the grid (70 bar) and raising of gas pressure to 50 bar in methanol synthesis (IBB only), but it only accounts for 5.3% of total electrical consumption in SAB and 6% in IBB. Compression energy requirements in the SAB process amount to 0.41 kWh/Nm^3_{bSNG} and compare to 0.98 kWh/Nm^3_{bSNG} estimated in our previous assessment of a biomass-to-biomethane process including catalytic WGS at 15 bar (a) [11]. Such results suggest that using low-pressure syngas conditioning processes to increase the syngas stoichiometric modulus by extracting CO_2 is more beneficial than hydrogen-generating reforming processes run at higher pressures, when considering specific energy consumption before electrolysis, and they deliver a syngas quality compatible with biomethanation [73]. Therefore, low-pressure liquid scrubbing is an energetically favorable alternative to catalytic syngas conditioning in IGBEB processes, when large quantities of surplus renewable electricity are available and surplus high-temperature heat is unavailable.

3.2 Process economics

Table 13 displays a summary of project economic indicators for each process configuration, including purchased

Table 12 Summary of process energy balance

Process ID	Thermal efficiency %	Plant efficiency %	bSNG specific energy input kWh/Nm^3	bSNG specific energy input before electrolysis kWh/Nm^3
SAB	66.1	50.6	7.65	0.73
IBB	89.8	51.5	17.01	1.54

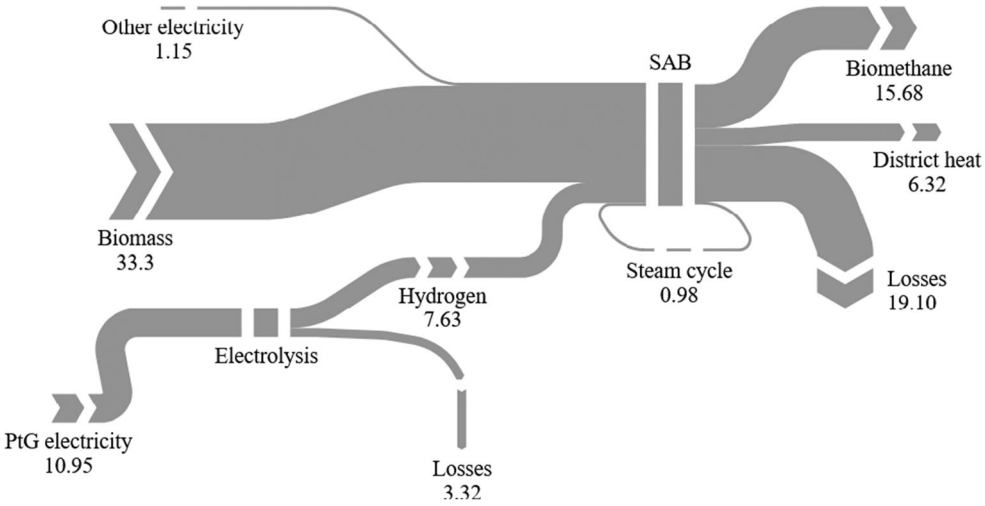

Fig. 8 Sankey diagram of energy flows (MW) in the SAB process.

equipment cost (PEC), total capital investment (TCI), direct yearly operating cost (D-OPEX), and total yearly operating cost (T-OPEX).

Figure 10 displays the breakdown of purchased equipment costs (PEC) for the two processes, indicating that large-scale electrolysis dominates the investment costs for the IBB process (37%), while it is the second PEC contributor (23%) in SAB, after gasification (39%). The size of the electrolysis plant in the SAB process is 11 MW, which is comparable with the size of the currently largest alkaline electrolysis (AE) plant worldwide [55, 56], suggesting that the operation of a similar system would be possible at the present technological readiness of AE. The electrolysis throughput required in the IBB process, instead, is approximately 24 MW, which would still represent a very large size plant, with limited feasibility. The next most capital-intensive plant section is biomethanation in both processes, while biomethanol synthesis and purification only contribute to 4% of PEC in the IBB process, indicating that the greatest CAPEX barrier of a process with carbon utilization is represented by large-scale electrolysis.

Figure 11 displays the breakdown of direct operating costs for the two processes. Biomass represents the greatest cost share in SAB (58%) and the second largest contributor (36%) in IBB, while PtG electricity is the largest OPEX component in IBB (48%) and the second largest component in SAB (34%). This highlights how the cost of electricity and biomass are the fundamental bottlenecks to the feasibility of IBGEB processes, as we previously demonstrated [11]. The role attributed to electrolysis is in line with various studies that recently identified it as the main CAPEX and OPEX contributor in similar process concepts, comprising CO_2-to-methane [74, 75], CO_2-to-methanol [76, 77], and CO_2-to-DME [78], although the same pattern has also been recognized across all the electrofuels mentioned and for electro-diesel and electro-gasoline [79].

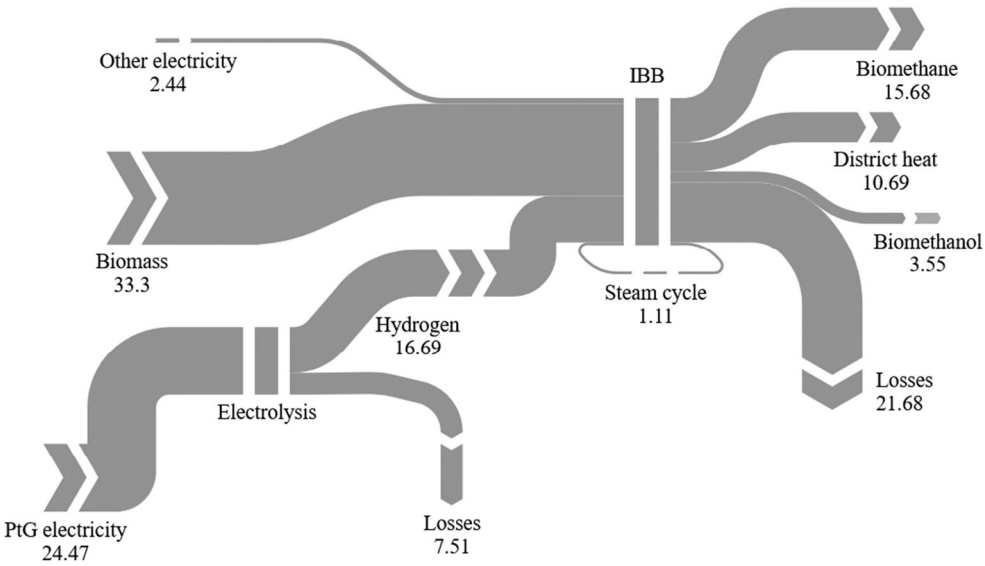

Fig. 9 Sankey diagram of energy flows (MW) in the IBB process

Table 13 Summary of project economic indicators

Process ID	PEC M€	TCI	D-OPEX M€/year	T-OPEX
SAB	32.3	125.5	9.8	16.2
IBB	45.1	152.4	15.7	25.1

3.3 Minimum selling price variation

As displayed by Table 14, the SAB process can produce biomethane at a MSP of 2.38 €/Nm^3, which is 11% lower than we previously estimated for a gasification-electrolysis-biomethanation process with catalytic water-gas shift [11] at an IRR of 7% (10% in this study), and approximately 170% higher than estimated by Michailos et al. [10] for a process without electrolysis. The lower MSP is made possible by a yearly side revenue of 3.9 M€ earned from district heat exports. However, despite having a positive effect on compression energy consumption, as described above, the absence of WGS needs compensation by means of high hydrogen flow rates and has thus a strong impact on MSP.

By selling renewable biomethanol to generate a further side revenue stream, the IBB process can deliver a biomethane MSP of 3.28 €/Nm^3, which corresponds to a 38% increase over the standalone process (SAB), indicating that the additional capital and operating costs generated by catalytic methanol synthesis and large-scale (24 MW) electrolysis outweigh the additional revenue earned at the current methanol selling price (275 €/t). It is possible to hypothesize that in future energy markets, a credit will be paid on any marginal renewable carbon that can be converted to fuel and stored in the short term, as is assumed in the two scenarios IBB(CC(25)) and IBB(CC(50)) in Table 14. However, the variation in bSNG selling price is negligible (− 1%) even in the presence of carbon credits on the renewable carbon stored as methanol, paid at a price equivalent to 25 €/t_{CO2} (IBB(CC25), which is close to the trading average in the European Emission Trading Scheme (ETS) [80]. The linear effect of carbon price on bSNG MSP is very limited (slope, 0.04 c€ · t_{CO2}/Nm^3/€), and even at a carbon price of 50 €/t_{CO2} (IBB(CC50)), the MSP only decreases by approximately 1% (3.26 €/Nm^3). In fact, the theoretical carbon credit prices that would generate an MSP equal to the natural gas consumer price in Europe (0.5 €/Nm3, Table 15), or the MSP of bSNG in the SAB process (2.38 €/Nm^3), were calculated at extreme rates of 5297 €/t_{CO2} and 1718 €/t_{CO2}, respectively, under the conditions considered. This demonstrates that, for the process analyzed, carbon utilization requires substantially larger CO_2 flows in order to have any meaningful impacts on process economics. As a result of the process economic indicators estimated, the MSP of standalone bSNG (SAB) is still 230% higher than the subsidized price of biomethane from anaerobic digestion of waste in Italy, granted by the application of the EU Renewable Energy Directive (RED 2009/28/EC) (Table 15).

3.4 Price gap of bSGN in biomass-to-biomethane processes

Figure 12 and 13 display the results of a sensitivity analysis on the cost of grid gas renewability by showing the monetary value of the government subsidy that would be required to match the bSNG price gap under parameter variation.

As expected from the breakdown of direct OPEX, the price gap is largely influenced by the variation in surplus energy cost and biomass cost (Fig. 12). The highest C_{biom} (200 €/t_{dry}, + 100% on base case) and the highest C_{PtG} (0.11 €/kWh, + 200% on base case) generate a 44% increase in MSP. However, in the case of zero-cost biomass, as in the hypothesis of waste lignocellulosic biomass, and zero-cost surplus energy, under the hypothesis of an energy system with a very high electrification level, the required subsidy would be 0.13 €/kWh_{bSNG}, which is 550% higher than the current market

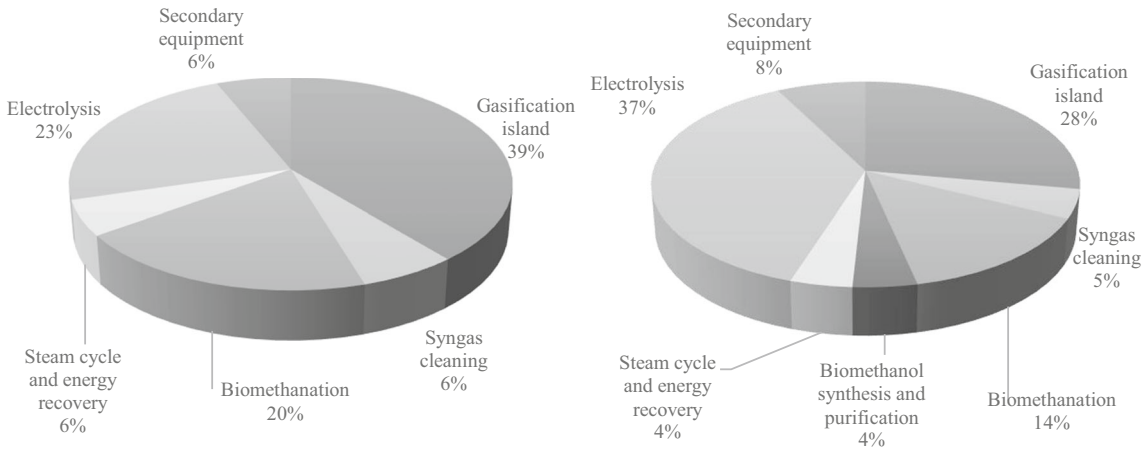

Fig. 10 Breakdown of purchased equipment cost (PEC) for the SAB (left) and the IBB (right) processes

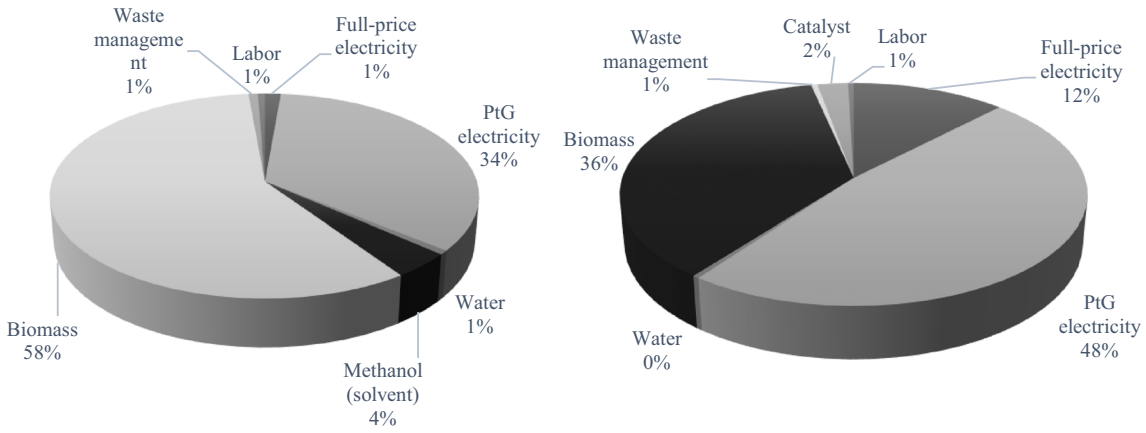

Fig. 11 Direct operating cost breakdown for the SAB (left) and the IBB (right) processes

price gap of both biomethane from AD (approximately 0.04 €/kWh). This indicates that subsidizing biomass-to-biomethane plants through the existing decarbonization financial support would be insufficient under any currently plausible techno-economic assumptions. The strategic nature of decentralized bSNG production along with its energy storage role would need to be factored into local energy policies to support biomass-to-biomethane developments through higher fiscal incentives in the future. The price gap achievable through integrated carbon utilization and biomethanol synthesis (IBB, Fig. 13) is higher than in SAB, although it is little influenced by biomethanol selling prices, demonstrating that the feasibility of such integrated biomethane-biomethanol process is ultimately cost-constrained, due to the CAPEX and OPEX intensity of electrolytic hydrogen. In fact, only a 38% increase in bSNG MSP is observed for $P_{bMeOH} = 0$ (−100%) when $C_{PtG} = 0.11$ €/kWh (+200%). Consequently, the bSNG price gap under the best-case assumptions for the cost

Table 14 Summary of main economic streams and bSNG minimum selling price for the two processes

Process ID	ACC	OPEX	Side Revenues				bSNG MSP
			District Heat	bMeOH	Carbon credits	Total	
	€/year						€/Nm$^3_{bSNG}$
SAB	15,362,766	16,222,193	3,875,977			3,875,977	2.38
IBB	18,668,414	25,128,247	6,555,056	1,035,689		7,590,745	3.28
IBB(CC25)	18,668,414	25,128,247	6,555,056	1,035,689	182,032	7,772,778	3.27
IBB(CC50)	18,668,414	25,128,247	6,555,056	1,035,689	364,065	7,954,810	3.26

Table 15 Summary of price comparisons between bSNG from SAB and biomethane from AD

Product type	Description	Price on product basis €/Nm^3	Price on energy basis €/kWh
bSNG from SAB	SAB process in this study	2.38	0.22
Biomethane from AD of waste and by-products	Anaerobic digestion of waste and by-products with biogas upgrading[a]	0.72[b]	0.07[c]
European natural gas	Grid natural gas for non-household consumers in EU28	-	0.03
Incentive required	Price gap between bSNG (SAB process) and natural gas	1.88	0.17

[a] Inclusive of average natural gas wholesale market price and advanced biofuel incentive (64.5 €/MWh)

[b] Based on a 3-month average wholesale market price of 0.01 €/kWh, January–March 2020 [81]

[c] Based on a biomethane LHV of 10.9 kWh/Nm^3

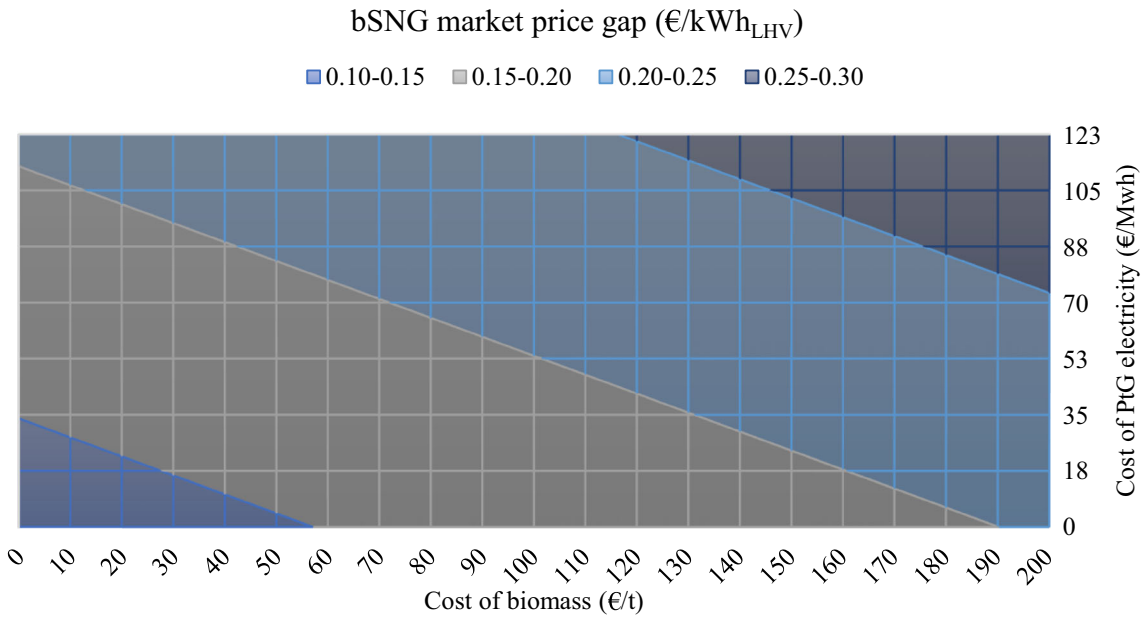

Fig. 12 Variation in the cost of gas grid renewability for the SAB process under varying biomass and PtG electricity costs

of energy (C_{PtG} = 0 (− 100% on base case)) and for the price of biomethanol (P_{bMeOH} = 500 €/t (+ 100% on base case)) is 0.25 €/kWh$_{bSNG}$. This indicates that, compared to SAB, carbon utilization for methanol synthesis would require an even larger fiscal support to reach financial competitiveness. Therefore, greater subsidization would be required in an IBB scenario, where a premium price would be needed in order sustain the role of biomethanol in enabling the development of localized biochemical value chains.

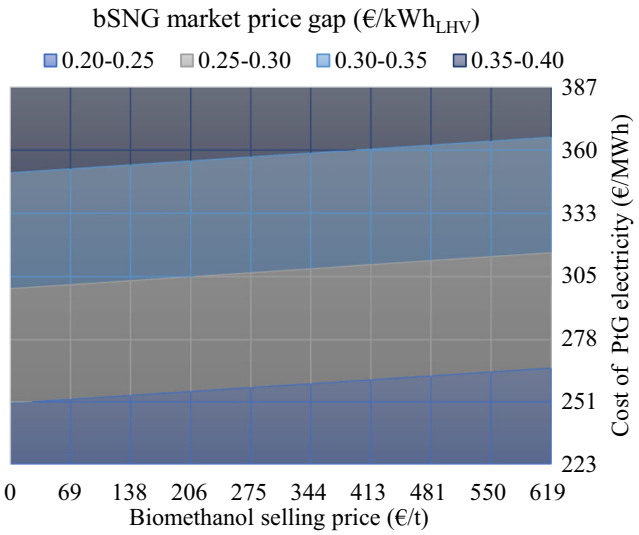

Fig. 13 Variation in the cost of gas grid renewability for the IBB process under varying biomethanol selling prices and PtG electricity costs at a constant biomass cost of 100 €/t$_{dry}$

3.5 Plant size competitiveness

The supply-side competitiveness of the biorenewable commodities considered (bSNG and bMeOH) is also affected by the production capacities achievable by the two processes in comparison with existing commercial processes in Europe (Table 16). Both processes analyzed can deliver approximately three times the bSNG capacity of a typical anaerobic digestion plant currently in operation or under construction in Europe (500 Nm^3/h). The IBB process can deliver additional 11 t bMeOH/day, equivalent to the production capacity of the George Olah pilot plant, which corresponds to approximately 0.2% of the capacity of an average European plant producing methanol from natural gas. With its current output, the George Olah plant is expected to satisfy approximately about 2.5% of the total gasoline market in Iceland [86], indicating that this scale would be appropriate for the supply of renewable methanol as fuel or as chemical feedstock in decentralized supply chains.

4 Conclusions

In this study, we carried out the techno-economic modeling of two processes comprising integrated biomass gasification, electrolysis, and syngas biomethanation (IBGEB) with combined heat and power recovery. The first process operates standalone biomethanation of syngas with the aid of water electrolysis and can produce approximately 38,000 Nm^3 of bSNG per day, with a total plant efficiency of 50.6%. The second process (integrated biomethane-biomethanol, IBB) exploits the unconverted carbon stream from the biomethanation

Table 16 Summary of typical plant sizes per type of product

Product type	Production process	Production capacity	Reference
Biomethane	Anaerobic digestion of waste	500 Nm^3/h	[82]
Biomethanol	Catalytic CO_2 hydrogenation (George Olah pilot plant)	11 t/day	[83]
	Catalytic CO_2 hydrogenation (MefCO_2 pilot plant)	1 t/day	[84]
Fossil-based methanol	Steam reforming of natural gas and syngas hydrogenation	5000 t/day	[85]

process to recover energy and synthesize methanol via direct catalytic CO_2 hydrogenation. In addition to the same bSNG output, the IBB process can produce 11 t/day of biomethanol, at a 99% purity. The selection of low-pressure liquid scrubbing processes in syngas conditioning upstream of biomethanation brings energy efficiency benefits compared to a catalytic WGS train, delivering a 64% decrease in specific energy consumption per bSNG unit volume, if electrolysis is neglected. The MSP of bSNG in the SAB process is 2.38 €/Nm^3, which is more than three times the magnitude of the subsidized price currently paid to biomethane from anaerobic digestion under the RED in Italy. The integrated production of biomethanol shows little global energy efficiency gains in comparison with SAB (51.7%) due to the large increase in electrolytic hydrogen demand, but it shows a substantial improvement of biomass-to-fuel carbon efficiency (33 vs. 26%). The integration of biomethanol production into the process generates high additional capital and operating costs, mainly due to the large additional electrolysis size required. As a result, the IBB process brings an increase in bSNG MSP of 76%, even with carbon credits on the additional carbon stored as fuel and does not improve bSNG feasibility in the absence of very intensive subsidization. The levels of subsidization required for the two processes exceed 0.13 €/kWh_{bSNG} for SAB and 0.25 €/kWh_{bSNG} for IBB under the most optimistic OPEX assumptions and suggest that government support for the strategic nature of these biorenewable commodities would be needed to complement existing decarbonization financial incentives. Despite its limited economic competitiveness, the IBB process would be competitive with existing renewable gas production plants, in terms of bSNG production capacity and could be adequate in supplying methanol to a decentralized biorenewable supply chain.

Supplementary Information The online version contains supplementary material available at https://doi.org/10.1007/s13399-020-01178-y.

Funding Open Access funding provided by Libera Università di Bolzano within the CRUI-CARE Agreement.

References

1. Rauch R, Hrbek J, Hofbauer H (2015) Biomass gasification for synthesis gas production and applications of the syngas. Adv Bioenergy Sustain Chall 73–91. https://doi.org/10.1002/9781118957844.ch7
2. Ptasinski KJ (2015) Bioenergy systems. Effic. Biomass Energy
3. Rönsch S, Schneider J, Matthischke S et al (2016) Review on methanation – from fundamentals to current projects. Fuel 166:276–296. https://doi.org/10.1016/J.FUEL.2015.10.111
4. IEA (2017) World Energy Outlook 2017
5. Wulf C, Linßen J, Zapp P (2018) Review of power-to-gas projects in Europe. Energy Procedia 155:367–378. https://doi.org/10.1016/j.egypro.2018.11.041
6. Karl J, Neubert M (2017) Production of substitute natural gas: thermochemical methods
7. Grimalt-Alemany A, Skiadas IV, Gavala HN (2018) Syngas biomethanation: state-of-the-art review and perspectives. Biofuels Bioprod Biorefin 12:139–158. https://doi.org/10.1002/bbb.1826
8. Lehner M, Tichler R, Steinmüller H, Koppe M (2014) The power-to-gas concept. In: Power-to-Gas: Technology and Business Models. Springer International Publishing, Cham, pp 7–17
9. Lehner M, Tichler R, Steinmüller H, Koppe M (2014) Methanation. In: Power-to-Gas: Technology and Business Models. Springer International Publishing, Cham, pp 41–61
10. Michailos S, Emenike O, Ingham D et al (2019) Methane production via syngas fermentation within the bio-CCS concept: a techno-economic assessment. Biochem Eng J 150:107290. https://doi.org/10.1016/j.bej.2019.107290
11. Menin L, Vakalis S, Benedetti V et al (2020) Techno-economic assessment of an integrated biomass gasification, electrolysis, and syngas biomethanation process. Biomass Convers Biorefinery. https://doi.org/10.1007/s13399-020-00654-9
12. Michailos S, Walker M, Moody A et al (2020) Biomethane production using an integrated anaerobic digestion, gasification and CO2 biomethanation process in a real waste water treatment plant: a techno-economic assessment. Energy Convers Manag 209:112663. https://doi.org/10.1016/j.enconman.2020.112663
13. Olah GA, Goeppert A, Prakash GKS (2009) Methanol-based chemicals, synthetic hydrocarbons and materials. In: Beyond Oil and Gas: The Methanol Economy. John Wiley & Sons, Ltd, pp 279–288
14. Olah GA, Goeppert A, Prakash GKS (2009) Methanol and dimethyl ether as fuels and energy carriers. In: Beyond Oil and Gas: The

Methanol Economy. Wiley-VCH Verlag GmbH & Co. KGaA, Weinheim, pp 185–231
15. Wang SW, Li DX, Ruan WB et al (2018) A techno-economic review of biomass gasification for production of chemicals. Energy Sources, Part B Econ Plan Policy 13:351–356. https://doi.org/10.1080/15567249.2017.1349212
16. Simakov DSA (2017) Thermocatalytic conversion of CO2. In: In: Renewable Synthetic Fuels and Chemicals from Carbon Dioxide: Fundamentals, Catalysis, Design Considerations and Technological Challenges. Springer International Publishing, Cham, pp 1–25
17. Anwar MN, Fayyaz A, Sohail NF et al (2020) CO2 utilization: turning greenhouse gas into fuels and valuable products. J Environ Manag 260:110059. https://doi.org/10.1016/j.jenvman.2019.110059
18. Bos MJ, Kersten SRA, Brilman DWF (2020) Wind power to methanol: renewable methanol production using electricity, electrolysis of water and CO2 air capture. Appl Energy 264:114672. https://doi.org/10.1016/j.apenergy.2020.114672
19. Rabaçal M, Ferreira AF, Silva CAM, Editors MC (2017) Biorefineries targeting energy, high value products and waste valorisation. Lect Notes Energy 57:307. https://doi.org/10.1007/978-3-319-48288-0
20. Araya SS, Liso V, Cui X et al (2020) A review of the methanol economy: the fuel cell route. Energies 13:596. https://doi.org/10.3390/en13030596
21. Moioli E, Mutschler R, Züttel A (2019) Renewable energy storage via CO2 and H2 conversion to methane and methanol: assessment for small scale applications. Renew Sust Energ Rev 107:497–506. https://doi.org/10.1016/j.rser.2019.03.022
22. Porté H, Kougias PG, Alfaro N et al (2019) Process performance and microbial community structure in thermophilic trickling biofilter reactors for biogas upgrading. Sci Total Environ 655:529–538. https://doi.org/10.1016/j.scitotenv.2018.11.289
23. Rachbauer L, Voitl G, Bochmann G, Fuchs W (2016) Biological biogas upgrading capacity of a hydrogenotrophic community in a trickle-bed reactor. Appl Energy 180:483–490. https://doi.org/10.1016/j.apenergy.2016.07.109
24. Bassani I, Kougias PG, Treu L et al (2017) Optimization of hydrogen dispersion in thermophilic up-flow reactors for ex situ biogas upgrading. Bioresour Technol 234:310–319. https://doi.org/10.1016/j.biortech.2017.03.055
25. Thema M, Bauer F, Sterner M (2019) Power-to-gas: electrolysis and methanation status review. Renew Sust Energ Rev 112:775–787. https://doi.org/10.1016/j.rser.2019.06.030
26. Vo TTQ, Wall DM, Ring D et al (2018) Techno-economic analysis of biogas upgrading via amine scrubber, carbon capture and ex-situ methanation. Appl Energy 212:1191–1202. https://doi.org/10.1016/j.apenergy.2017.12.099
27. Kassem N, Hockey J, Lopez C et al (2020) Integrating anaerobic digestion, hydrothermal liquefaction, and biomethanation within a power-to-gas framework for dairy waste management and grid decarbonization: a techno-economic assessment. Sustain Energy Fuels 4:4644–4661. https://doi.org/10.1039/d0se00608d
28. Asimakopoulos K, Gavala HN, Skiadas IV (2019) Biomethanation of syngas by enriched mixed anaerobic consortia in trickle bed reactors. Waste Biomass Valoriz 11:495–512. 0:0. https://doi.org/10.1007/s12649-019-00649-2
29. Haro P, Johnsson F, Thunman H (2016) Improved syngas processing for enhanced Bio-SNG production: a techno-economic assessment. Energy 101:380–389. https://doi.org/10.1016/j.energy.2016.02.037
30. Alamia A, Larsson A, Breitholtz C, Thunman H (2017) Performance of large-scale biomass gasifiers in a biorefinery, a state-of-the-art reference. Int J Energy Res 41:2001–2019. https://doi.org/10.1002/er.3758
31. Yun HAH, Ramírez-Solís S, Dupont V (2020) Bio-CH4 from palm empty fruit bunch via pyrolysis-direct methanation: full plant model and experiments with bio-oil surrogate. J Clean Prod 244:118737. https://doi.org/10.1016/j.jclepro.2019.118737
32. Guiot SR, Cimpoia R, Carayon G (2011) Potential of wastewater-treating anaerobic granules for biomethanation of synthesis gas. Environ Sci Technol 45:2006–2012. https://doi.org/10.1021/es102728m
33. François J, Mauviel G, Feidt M et al (2013) Modeling of a biomass gasification CHP plant: influence of various parameters on energetic and exergetic efficiencies. Energy Fuel 27:7398–7412. https://doi.org/10.1021/ef4011466
34. Alamia A, Thunman H, Seemann M (2016) Process simulation of dual fluidized bed gasifiers using experimental data. Energy Fuel 30:4017–4033. https://doi.org/10.1021/acs.energyfuels.6b00122
35. Duret A, Friedli C, Maréchal F (2005) Process design of Synthetic Natural Gas (SNG) production using wood gasification. J Clean Prod 13:1434–1446. https://doi.org/10.1016/j.jclepro.2005.04.009
36. Li XT, Grace JR, Lim CJ et al (2004) Biomass gasification in a circulating fluidized bed. Biomass Bioenergy 26:171–193. https://doi.org/10.1016/S0961-9534(03)00084-9
37. Francois J, Abdelouahed L, Mauviel G et al (2013) Detailed process modeling of a wood gasification combined heat and power plant. Biomass Bioenergy 51:68–82. https://doi.org/10.1016/j.biombioe.2013.01.004
38. Abdelouahed L, Authier O, Mauviel G et al (2012) Detailed modeling of biomass gasification in dual fluidized bed reactors under aspen plus. Energy Fuel 26:3840–3855. https://doi.org/10.1021/ef300411k
39. Zhang Z, Pang S (2019) Experimental investigation of tar formation and producer gas composition in biomass steam gasification in a 100 kW dual fluidised bed gasifier. Renew Energy 132:416–424. https://doi.org/10.1016/j.renene.2018.07.144
40. Karl J, Pröll T (2018) Steam gasification of biomass in dual fluidized bed gasifiers: a review. Renew Sust Energ Rev 98:64–78. https://doi.org/10.1016/j.rser.2018.09.010
41. Gatti M, Martelli E, Marechal F, Consonni S (2014) Review, modeling, heat integration, and improved schemes of Rectisol®-based processes for CO2 capture. Appl Therm Eng 70:1123–1140. https://doi.org/10.1016/j.applthermaleng.2014.05.001
42. Schefflan R (2011) Teach yourself the basics of Aspen Plus
43. (2000) Aspen Plus ® User Guide. 936
44. Magli F, Capra F, Gatti M, Martelli E (2018) Process selection, modelling and optimization of a water scrubbing process for energy-self-sufficient biogas upgrading plants. Sustain Energy Technol Assessments 27:63–73. https://doi.org/10.1016/j.seta.2018.02.001
45. Asimakopoulos K, Łężyk M, Grimalt-Alemany A et al (2020) Temperature effects on syngas biomethanation performed in a trickle bed reactor. Chem Eng J 393:124739. https://doi.org/10.1016/j.cej.2020.124739
46. Ullrich T, Lindner J, Bär K et al (2018) Influence of operating pressure on the biological hydrogen methanation in trickle-bed reactors. Bioresour Technol 247:7–13. https://doi.org/10.1016/j.biortech.2017.09.069
47. Anicic B, Trop P, Goricanec D (2014) Comparison between two methods of methanol production fromcarbon dioxide. Energy 77:279–289. https://doi.org/10.1016/j.energy.2014.09.069
48. Gallucci F, Paturzo L, Basile A (2004) An experimental study of CO2 hydrogenation into methanol involving a zeolite membrane reactor. Chem Eng Process Process Intensif 43:1029–1036. https://doi.org/10.1016/j.cep.2003.10.005
49. Elkamel A, Reza Zahedi G, Marton C, Lohi A (2009) Optimal fixed bed reactor network configuration for the efficient recycling of CO2 into methanol. Energies 2:180–189. https://doi.org/10.3390/en20200180

50. Centi G, Perathoner S (2009) Opportunities and prospects in the chemical recycling of carbon dioxide to fuels. Catal Today 148: 191–205. https://doi.org/10.1016/j.cattod.2009.07.075
51. Van-Dal ÉS, Bouallou C (2013) Design and simulation of a methanol production plant from CO2 hydrogenation. J Clean Prod 57: 38–45. https://doi.org/10.1016/j.jclepro.2013.06.008
52. Crivellari A, Cozzani V, Dincer I (2019) Exergetic and exergoeconomic analyses of novel methanol synthesis processes driven by offshore renewable energies. Energy 187:115947. https://doi.org/10.1016/j.energy.2019.115947
53. Matzen M, Alhajji M, Demirel Y (2015) Chemical storage of wind energy by renewable methanol production: feasibility analysis using a multi-criteria decision matrix. Energy 93:343–353. https://doi.org/10.1016/j.energy.2015.09.043
54. Rahmatmand B, Rahimpour MR, Keshavarz P (2019) Introducing a novel process to enhance the syngas conversion to methanol over Cu/ZnO/Al2O3 catalyst. Fuel Process Technol 193:159–179. https://doi.org/10.1016/j.fuproc.2019.05.014
55. Lee A (2020) Japan completes construction of world's largest green hydrogen project. In: Institutre Energy Econ. Financ. Anal. https://ieefa.org/japan-completes-construction-of-worlds-largest-green-hydrogen-project/
56. (2018) Construction begins on Fukushima Hydrogen Energy Research Field. Fuel Cells Bull 2018:9. https://doi.org/10.1016/S1464-2859(18)30332-8
57. Guillet N, Millet P (2015) Alkaline water electrolysis. In: Hydrogen Production. John Wiley & Sons, Ltd, pp 117–166
58. Schalenbach M, Zeradjanin AR, Kasian O et al (2018) A perspective on low-temperature water electrolysis - challenges in alkaline and acidic technology. Int J Electrochem Sci 13:1173–1226. https://doi.org/10.20964/2018.02.26
59. Ayers K, Danilovic N, Ouimet R et al (2019) Perspectives on low-temperature electrolysis and potential for renewable hydrogen at scale. Annu Rev Chem Biomol Eng 10:219–239. https://doi.org/10.1146/annurev-chembioeng-060718-030241
60. Holmgren KM (2015) Investment cost estimates for gasification-based biofuel production systems
61. Karimi M, Hillestad M, Svendsen HF (2011) Capital costs and energy considerations of different alternative stripper configurations for post combustion CO2 capture. Chem Eng Res Des 89: 1229–1236. https://doi.org/10.1016/j.cherd.2011.03.005
62. Liu X, Yang S, Hu Z, Qian Y (2015) Simulation and assessment of an integrated acid gas removal process with higher CO2 capture rate. Comput Chem Eng 83:48–57. https://doi.org/10.1016/j.compchemeng.2015.01.008
63. Ferella F, Cucchiella F, D'Adamo I, Gallucci K (2019) A techno-economic assessment of biogas upgrading in a developed market. J Clean Prod 210:945–957. https://doi.org/10.1016/j.jclepro.2018.11.073
64. Albrecht FG, König DH, Baucks N, Dietrich R-UU (2017) A standardized methodology for the techno-economic evaluation of alternative fuels – a case study. Fuel 194:511–526. https://doi.org/10.1016/j.fuel.2016.12.003
65. Brown RC, Brown TR (2014) Economics of biorenewable resources. In: Biorenewable Resources. John Wiley & Sons, Ltd, pp 287–326
66. Methanex Corporation (2020) Pricing. https://www.methanex.com/our-business/pricing. Accessed 8 Oct 2020
67. Gruppo Hera (2020) Prezzi del servizio teleriscaldamento. https://www.gruppohera.it/binary/hr_clienti/casa_teleriscaldamento_tariffe_feb15/2020_Bologna_Modulo_TARIFFE_01_07_2020.1596527623.pdf. Accessed 12 Oct 2020
68. Alperia (2020) La nostra offerta in dettaglio. https://www.alperia.eu/la-mia-casa/telecalore/calore-bolzano.html. Accessed 12 Oct 2020
69. a2a (2020) Prezzi fornitura teleriscaldamento, Bergamo e Milano. https://www.a2acaloreservizi.eu/home/cms/a2a_caloreservizi/area_clienti/documenti/Prezzi-TLR-MILANO-BERGAMO-01_ott_2020.pdf. Accessed 12 Oct 2020
70. Eurostat (2020) Gas prices for non-household consumers - bi-annual data (from 2007 onwards). https://appsso.eurostat.ec.europa.eu/nui/show.do?dataset=nrg_pc_203&lang=en. Accessed 8 Apr 2020
71. Alsayegh S, Johnson JR, Ohs B, Wessling M (2019) Methanol production via direct carbon dioxide hydrogenation using hydrogen from photocatalytic water splitting: process development and techno-economic analysis. J Clean Prod 208:1446–1458. https://doi.org/10.1016/j.jclepro.2018.10.132
72. Pérez-Fortes M, Schöneberger JC, Boulamanti A, Tzimas E (2016) Methanol synthesis using captured CO2 as raw material: techno-economic and environmental assessment. Appl Energy 161:718–732. https://doi.org/10.1016/j.apenergy.2015.07.067
73. Guiot S (2013) Bio-upgrading of syngas into methane. In: In: Proceedings of the 13th World Congress on Anaerobic Digestion. Santiago de Compostela, Spain
74. Chauvy R, Dubois L, Lybaert P et al (2020) Production of synthetic natural gas from industrial carbon dioxide. Appl Energy 260: 114249. https://doi.org/10.1016/j.apenergy.2019.114249
75. Peters R, Baltruweit M, Grube T et al (2019) A techno economic analysis of the power to gas route. J CO2 Util 34:616–634. https://doi.org/10.1016/j.jcou.2019.07.009
76. Adnan MA, Kibria MG (2020) Comparative techno-economic and life-cycle assessment of power-to-methanol synthesis pathways. Appl Energy 278:115614. https://doi.org/10.1016/j.apenergy.2020.115614
77. Nyári J, Magdeldin M, Larmi M et al (2020) Techno-economic barriers of an industrial-scale methanol CCU-plant. J CO2 Util 39:101166. https://doi.org/10.1016/j.jcou.2020.101166
78. Michailos S, McCord S, Sick V et al (2019) Dimethyl ether synthesis via captured CO2 hydrogenation within the power to liquids concept: a techno-economic assessment. Energy Convers Manag 184:262–276. https://doi.org/10.1016/j.enconman.2019.01.046
79. Brynolf S, Taljegard M, Grahn M, Hansson J (2018) Electrofuels for the transport sector: a review of production costs. Renew Sust Energ Rev 81:1887–1905
80. Bloomberg (2020) ECX emissions (ICE). https://www.bloomberg.com/quote/MO1:COM. Accessed Apr 2020
81. GME (2020) Statistiche - comunicazioni DM 2.03.2018 biometano. https://www.mercatoelettrico.org/It/Statistiche/Gas/ComBiometanoNew.aspx. Accessed 9 Apr 2020
82. Scarlat N, Dallemand JF, Fahl F (2018) Biogas: developments and perspectives in Europe. Renew Energy 129:457–472. https://doi.org/10.1016/j.renene.2018.03.006
83. Hobson C, Marquez C (2018) Renewable methanol report. Accessed Apr 2020
84. MefCO2 (2019) Project progress. http://www.mefco2.eu/project_progress.php. Accessed Apr 2020
85. Fraile D, Lanoix J-C, Maio P, et al (2015) Overview of the market segmentation for hydrogen across potential customer groups, based on key application areas
86. chemicals-technology.com (2012) George Olah CO2 to renewable methanol plant , Reykjanes. In: Verdict Media Ltd. https://www.chemicals-technology.com/projects/george-olah-renewable-methanol-plant-iceland/. Accessed Apr 2020